

## **Supporting Information**

### **Arylruthenium(III) Porphyrin-Catalyzed C–H Oxidation and Epoxidation at Room Temperature and [Ru<sup>V</sup>(Por)(O)(Ph)] Intermediate by Spectroscopic Analysis and DFT Calculations**

Ka-Pan Shing,<sup>†</sup> Bei Cao,<sup>†</sup> Yungen Liu,<sup>†</sup> Hung Kay Lee,<sup>‡</sup> Ming-De Li,<sup>†</sup> David Lee Phillips,<sup>†</sup> Xiao-Yong Chang,<sup>†</sup> and Chi-Ming Che<sup>†,§,\*</sup>

<sup>†</sup>Department of Chemistry and State Key Laboratory of Synthetic Chemistry, The University of Hong Kong, Pokfulam Road, Hong Kong, China

<sup>‡</sup>Department of Chemistry, The Chinese University of Hong Kong, Shatin, New Territories, Hong Kong, China

<sup>§</sup>HKU Shenzhen Institute of Research and Innovation, Shenzhen 518053, China

E-mail: cmche@hku.hk

## Table of Contents

---

<b>Abbreviations</b>	S4
<b>Experimental Section</b>	S4
Material and Instrumentation	S4
Synthesis and Characterization of Ru(II), Ru(III), Ru(IV) and Ru(VI) Porphyrins	S5
X-Ray Crystal Structure Determination	S7
UV-vis Spectroelectrochemistry Measurement	S7
General Procedure for [Ru <sup>III</sup> (Por)(Ph)(L)]-Catalyzed Epoxidation and C-H Oxidation	S7
Characterization of Organic Products	S8
Hammett Plot	S9
Kinetic Measurements	S9
X-Band EPR Spectroscopy	S9
ESI-MS	S10
Preparation of <sup>18</sup> O-Labelled <i>m</i> -CPBA	S10
Resonance Raman Spectroscopy	S10
Computational Details	S12
<b>References</b>	S13
<b>Table S1.</b> Crystallographic Data for Complexes <b>1–3</b>	S15
<b>Table S2.</b> Catalyst Screening for the Oxidation of 1-Decene with [ <sup>n</sup> Bu <sub>4</sub> N]IO <sub>4</sub>	S16
<b>Table S3.</b> Data Used to Plot the Hammett Correlation for <b>1</b> -Catalyzed C-H Oxidation of <i>para</i> -Substituted Ethylbenzenes with <i>m</i> -CPBA	S17
<b>Table S4.</b> Rate Constants ( <i>k</i> <sub>2</sub> ) for the Oxidation of Hydrocarbons by ‘ <b>1</b> + <i>m</i> -CPBA (1 equiv)’	S18
<b>Table S5.</b> Comparison of the <i>g</i> Tensors for Ru Species with <i>S</i> = 1/2	S19
<b>Figure S1.</b> ESI-MS Spectra of <b>1</b> and <b>2</b>	S20
<b>Figure S2.</b> UV-vis Spectral Change of the Electrochemical Oxidation of <b>2</b> at Constant Voltage (+0.5 V)	S21
<b>Figure S3.</b> UV-vis Spectral Changes for <b>1</b> + <i>m</i> -CPBA in CH <sub>2</sub> Cl <sub>2</sub>	S22
<b>Figure S4.</b> Simulated and Observed Isotopic Patterns for [Ru(TDCPP)(O)(Ph)] ( <b>A</b> ) and ‘95% [Ru(TDCPP)(Ph)( <sup>16</sup> O)] + 5% [Ru(TDCPP)(Ph)( <sup>18</sup> O)]’	S23
<b>Figure S5.</b> X-Band EPR Spectrum of <b>1</b> Recorded at 40 K	S24
<b>Figure S6.</b> Graphs Showing <i>k</i> <sub>obs</sub> of Hydrocarbon Oxidation by <b>1</b> vs Concentration of Hydrocarbons (298 K)	S25
<b>Figure S7.</b> Graphs Showing ln A-A <sub>∞</sub>   at 420 nm vs Time for Various Concentrations of Ethylbenzene	S27
<b>Figure S8.</b> Graphs Showing ln A-A <sub>∞</sub>   at 420 nm vs Time for Various Concentrations of Xanthene	S28
<b>Figure S9.</b> Graphs Showing ln A-A <sub>∞</sub>   at 420 nm vs Time for Various Concentrations of 9,10-Dihydroanthracene	S29
<b>Figure S10.</b> Graphs Showing ln A-A <sub>∞</sub>   at 420 nm vs Time for Various Concentrations of Fluorene	S30
<b>Figure S11.</b> Graphs Showing ln A-A <sub>∞</sub>   at 420 nm vs time for Various Concentrations of Methylcyclohexane	S31
<b>Figure S12.</b> Graphs Showing ln A-A <sub>∞</sub>   at 420 nm vs Time for Various Concentrations of Methylcyclohexane- <i>d</i> <sub>14</sub>	S32
<b>Figure S13.</b> Graphs Showing ln A-A <sub>∞</sub>   at 420 nm vs Time for Various Concentrations of 1-Phenylethanol	S33
<b>Figure S14.</b> Graphs Showing ln A-A <sub>∞</sub>   at 420 nm vs Time for Various Concentrations of 1-Phenylethanol- <i>d</i> <sub>10</sub>	S34

<b>Figure S15.</b> Graphs Showing $\ln A - A_\infty $ at 420 nm vs Time for Various Concentrations of 1-Decene	S35
<b>Figure S16.</b> Free Energy Surface of Hydroxylation of Methylcyclohexane by $[\text{Ru}^V(\text{TDCPP})(\text{O})(\text{Ph})]$	S36
<b>Figure S17.</b> TD-DFT Simulated UV-vis Spectra of $[\text{Ru}^V(\text{TDCPP})(\text{O})(\text{Ph})]$ , $[\text{Ru}^{VI}(\text{TDCPP})(\text{O})_2]$ , and $[\text{Ru}^{III}(\text{TDCPP})(\text{Ph})]$	S37
<b>Figure S18.</b> Graph Showing the Brønsted-Evans-Polanyi Relationship Cartesian Coordinates from DFT Calculations	S38 S39

---

## Abbreviations

**Cl<sub>2</sub>pyNO:** 2,6-dichloropyridine-*N*-oxide  
**m-CPBA:** *m*-chloroperoxybenzoic acid  
**CCl<sub>4</sub>:** carbon tetrachloride  
**TMSCl:** trimethylsilyl chloride  
**ESI-MS:** electrospray ionization mass spectrometry  
**N<sub>4</sub>OH:** bis[2-(2-pyridyl)ethyl][2-hydroxy-2-(2-pyridyl)ethyl]amine  
**OEP:** 2,3,7,8,12,13,17,18-octaethylporphyrinato(2-)  
**Oxone:** potassium peroxyomonosulfate, 2KHSO<sub>5</sub>·KHSO<sub>4</sub>·K<sub>2</sub>SO<sub>4</sub>  
**Por:** porphyrinato(2-)  
**qpy:** 2,2':6',2'':6'',2''':6'''-quinquepyridine  
**TDCPP:** 5,10,15,20-tetrakis(2,6-dichlorophenyl)porphyrinato(2-)  
**TDFPP:** 5,10,15,20-tetrakis(2,6-difluorophenyl)porphyrinato(2-)  
**TPP:** 5,10,15,20-tetraphenylporphyrinato(2-)  
**TMP:** 5,10,15,20-tetrakis(2,4,6-trimethylphenyl)porphyrinato(2-)  
**F<sub>20</sub>-TPP:** 5,10,15,20-tetrakis(pentafluorophenyl)porphyrinato(2-)

## Experimental Section

### Materials and Instrumentation

Anhydrous 1,4-dioxane and other reagents were purchased from Sigma-Aldrich and used without purification unless mentioned otherwise. Ru<sub>3</sub>(CO)<sub>12</sub> was purchased from Dieckmann. Acetonitrile and dichloromethane were freshly distilled with CaH<sub>2</sub> before use. Iodosylbenzene (PhI=O),<sup>1</sup> H<sub>2</sub>TDCPP,<sup>2a</sup> H<sub>2</sub>TDFPP,<sup>2b</sup> (*E*)-1-phenyl-1,3-diene,<sup>3</sup>  $\alpha$ -methyl- $\gamma$ -phenylallyl pivalate and  $\alpha$ -methyl- $\gamma$ -phenylallyl acetate<sup>4</sup> were synthesized according to literature methods. Merck silica gel 60 was used for flash column chromatography. <sup>1</sup>H and <sup>13</sup>C NMR spectra were recorded using a Bruker DPX400 or DPX300 spectrometer; the solvent CDCl<sub>3</sub> contains trimethylsilane (TMS) as an internal standard and all the chemical shifts were reported relative to TMS. Effective magnetic moments were measured by the Evans method. Cyclic voltammetry was carried out on a Princeton Applied Research Model 273A potentiostat/galvanostat coulometer with a three-electrode cell system (working electrode, glassy carbon; counter electrode, platinum wire; reference electrode: 0.1 M Ag/AgNO<sub>3</sub> in MeCN). UV-vis spectra were recorded on a Cary 8454 UV-vis spectrophotometer (Agilent Technologies). Positive-ion mode electron-impact (EI) mass spectra were recorded on a Thermo Scientific DFS high resolution

magnetic sector MS. Gas chromatography (GC-FID) measurements (% conversion and % yield) were performed by using a HP 5890 Series II with a flame ionization detector and a 3396 Series II integrator. GC-MS analysis was performed by Agilent Technologies 7890B GC system with 5977A MS detector. Bruker EMX EPR spectrometer with a variable-temperature helium flow cryostat system was used to record X-band EPR spectra at 7 K. Low-resolution and high-resolution ESI-MS (positive-ion mode) measurements were recorded on a Finnigan LCQ quadrupole ion trap mass spectrometer and a Waters Micromass Q-ToF Premier quadrupole time-of-flight tandem mass spectrometer, respectively.

### Synthesis and Characterization of Ru(II), Ru(III), Ru(IV) and Ru(VI) Porphyrins

#### Synthesis of [Ru<sup>II</sup>(Por)(CO)] (Por = TDCPP and TDFPP)

A 100-mL two-necked round-bottom flask was charged with 1,2,4-trichlorobenzene (50 mL), followed by degassing with argon for 15 min. After that, H<sub>2</sub>TDCPP or H<sub>2</sub>TDFPP (300 mg) was added to the degassed solution under argon. The reaction system was then purged continuously with argon and heated to 160–165 °C. 12 portions of Ru<sub>3</sub>(CO)<sub>12</sub> (25 mg each, totally 300 mg) were added to the reaction mixture (protected with argon flow) at a 15-min interval. After addition of the final portion, the mixture was allowed to stir for extra 1 h. The reaction mixture was then cooled to room temperature. [Ru<sup>II</sup>(Por)(CO)] was obtained by purification of the product through column chromatography on neutral alumina: with *n*-hexane (as eluent) to remove 1,2,4-trichlorobenzene, CH<sub>2</sub>Cl<sub>2</sub>/hexane to remove unreacted porphyrin, and CH<sub>2</sub>Cl<sub>2</sub>/acetone to elute the desired product.

#### Synthesis of [Ru<sup>VI</sup>(TDCPP)(O)<sub>2</sub>]

To a 100-mL round-bottom flask containing [Ru<sup>II</sup>(Por)(CO)] (200 mg) was added CH<sub>2</sub>Cl<sub>2</sub> (70 mL), followed by portionwise addition of *m*-CPBA (300 mg). After 5 min, the excess *m*-CPBA was removed by a short alumina column using CH<sub>2</sub>Cl<sub>2</sub> as eluent. The fast-moving brown band was collected and concentrated to dryness under vacuum at room temperature, giving the desired product as a purple solid.

#### Synthesis of [Ru<sup>IV</sup>(TDCPP)(Cl)<sub>2</sub>]

To a 100-mL two-necked round-bottom flask was added [Ru<sup>VI</sup>(TDCPP)(O)<sub>2</sub>] (200 mg). Under inert atmosphere, anhydrous CH<sub>2</sub>Cl<sub>2</sub> (70 mL) and trimethylsilyl chloride (0.5 mL) were sequentially added via syringes. The reaction mixture was stirred for 2 h and then concentrated to a smaller volume, followed by filtration and washing with diethyl ether to afford the title product.

### **Characterization of [Ru<sup>II</sup>(TDCPP)(CO)], [Ru<sup>IV</sup>(TDCPP)(Cl)<sub>2</sub>] and [Ru<sup>VI</sup>(TDCPP)(O)<sub>2</sub>]**

These complexes were characterized as reported previously.<sup>5</sup>

### **Characterization of [Ru<sup>II</sup>(TDFPP)(CO)]**

This complex was characterized as reported previously.<sup>6</sup>

### **Synthesis of [Ru<sup>III</sup>(TDFPP)(Cl)(THF)] (3)**

A mixture of [Ru<sup>II</sup>(TDFPP)(CO)] with CCl<sub>4</sub> was allowed to reflux in air overnight. After removal of the solvent, the desired product was obtained as a dark red solid by recrystallization from anhydrous THF/diethyl ether. Yield: 80%. <sup>1</sup>H NMR (CDCl<sub>3</sub>): δ -27.75 (H<sub>β</sub>, bs, 8H), 4.36 (H<sub>m'</sub>, d, 4H), 4.61 (H<sub>m</sub>, d, 4H), 6.09 (H<sub>p</sub>, 4H), 15.5 (OCH<sub>2</sub>CH<sub>2</sub>, bs, 4H) (OCH<sub>2</sub>CH<sub>2</sub> not observed); UV-vis (3.7 × 10<sup>-6</sup> M, CH<sub>2</sub>Cl<sub>2</sub>): λ<sub>max</sub> (log ε) 408 (5.32), 524 nm (4.31); ESI-MS (CH<sub>2</sub>Cl<sub>2</sub>): *m/z* 893.0 [M – THF]<sup>+</sup>, 858 [M – THF – Cl]<sup>+</sup>; Effective magnetic moment: 1.75 μ<sub>B</sub> (*S* = 1/2).

### **Synthesis of [Ru<sup>III</sup>(TDCPP)(Ph)(OEt<sub>2</sub>)] (1) and [Ru<sup>III</sup>(TDFPP)(Ph)(OH<sub>2</sub>)] (2)**

In a Schlenk flask, [Ru<sup>IV</sup>(TDCPP)Cl<sub>2</sub>] or [Ru<sup>III</sup>(TDFPP)(Cl)(THF)] (0.189 mmol) was added, followed by drying under vacuum. Under inert atmosphere, anhydrous toluene (4 mL) was added via syringe. The reaction flask was then immersed into an acetone/N<sub>2</sub>(l) bath. After that, 10 equiv of phenyllithium (1.6 M in diethyl ether) was slowly added into the mixture with vigorous stirring. The mixture was allowed to warm to room temperature, followed by stirring at room temperature for 30 min. Water (15 mL) was slowly added into the mixture via syringe under argon. The mixture was extracted with CH<sub>2</sub>Cl<sub>2</sub> (30 mL × 4) until the organic layer became colorless. The combined organic layer was then evaporated to dryness and loaded into a neutral alumina-packed column. The brown band was collected by eluting with CH<sub>2</sub>Cl<sub>2</sub>/hexane. The solvent was dried under vacuum to give a black solid.

**[Ru<sup>III</sup>(TDCPP)(Ph)(OEt<sub>2</sub>)] (1).** Yield: 66%. <sup>1</sup>H NMR (CDCl<sub>3</sub>): δ -102.50 (H<sub>o</sub>, bs, 2H), -75.00 (H<sub>p</sub>, bs, 2H), -30.71 (H<sub>β</sub>, bs, 8H), 4.77-4.79 (H<sub>m'</sub>, bs, 4H), 4.96-4.98 (H<sub>m</sub>, bs, 4H), 5.59-5.63 (H<sub>p</sub>, bs, 4H), 54.27 (H<sub>m</sub>, bs, 2H); ESI-MS (CH<sub>2</sub>Cl<sub>2</sub>): *m/z* 1067 [M – OEt<sub>2</sub>]<sup>+</sup>, 990 [M – OEt<sub>2</sub> – Ph]<sup>+</sup>; UV-vis (6.3 × 10<sup>-6</sup> M, CH<sub>2</sub>Cl<sub>2</sub>): λ<sub>max</sub> (log ε) 405 (5.10), 522 (4.11), 615 nm (sh, 3.79); Effective magnetic moment: 1.77 μ<sub>B</sub> (*S* = 1/2).

**[Ru<sup>III</sup>(TDFPP)(Ph)(OH<sub>2</sub>)] (2).** Yield: 73%. <sup>1</sup>H NMR (CDCl<sub>3</sub>): δ -103.40 (H<sub>o</sub>, bs, 2H), -76.30 (H<sub>p</sub>, bs, 2H), -30.57 (H<sub>β</sub>, bs, 8H), 4.25-4.27 (H<sub>m</sub>, bs, 4H), 4.50-4.52 (H<sub>m</sub>, bs, 4H), 5.74-5.78 (H<sub>p</sub>, bs, 4H), 54.23 (H<sub>m</sub>, bs, 2H); ESI-MS (CH<sub>2</sub>Cl<sub>2</sub>): *m/z* 935 [M – OH<sub>2</sub>]<sup>+</sup>, 859 [M – OH<sub>2</sub> – Ph]<sup>+</sup>; UV-vis (6.0 × 10<sup>-6</sup> M, CH<sub>2</sub>Cl<sub>2</sub>): λ<sub>max</sub> (log ε) 410 (5.07), 521 (4.12); Effective magnetic moment: 1.78 μ<sub>B</sub> (*S* = 1/2).

### X-Ray Crystal Structure Determination

A diffraction-quality crystal of **1** was obtained by slow diffusion of diethyl ether and hexane (1:1 v/v) into a dichloromethane solution of **1**. Similarly, slow diffusion of diethyl ether into a dichloromethane solution of **2** gave a diffraction-quality crystal of **2**. A diffraction-quality crystal of **3** was obtained by layering diethyl ether on the top of a tetrahydrofuran solution of the crude product obtained by refluxing [Ru<sup>II</sup>(TDFPP)(CO)] in CCl<sub>4</sub>. Each of the crystals was quickly mounted in a glass fiber and measured at a temperature of 100 K. The X-ray diffraction data were collected on a Bruker Proteum X8 diffractometer with monochromated Cu-Kα radiation. The Proteum2 program package was used for cell refinement and data reduction.<sup>7</sup> All structures were solved by direct methods using SHELXS and refined by full-matrix least-squares on |*F*<sup>2</sup>| algorithm (SHELXL)<sup>8</sup> using Olex2 program.<sup>9</sup> Some solvent molecules in the crystal structure of **2** were omitted using SQUEEZE routing of PLATON program as they were highly disordered and could not be resolved unambiguously.

### UV-vis Spectroelectrochemistry Measurement

Approximately 1.3 mL of CH<sub>2</sub>Cl<sub>2</sub> solution containing 6.8 × 10<sup>-5</sup> M of **2** and 0.1 M [<sup>n</sup>Bu<sub>4</sub>N]PF<sub>6</sub> was added to a batch-type UV cell designed for spectroelectrochemistry with 1 mm path length. After that, Pt gauze working electrode, Pt counter electrode and pseudo-reference electrode were connected to the same instrument used for cyclic voltammetry. The UV-vis spectra were recorded once a constant voltage (+0.5 V) was applied to the sample.

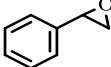
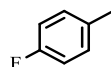
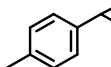
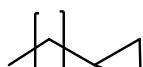
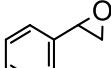
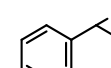
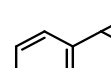
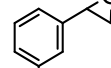
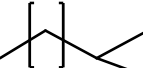
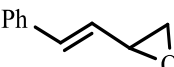
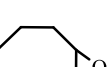
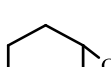
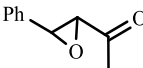
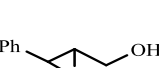
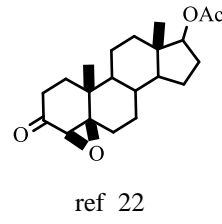
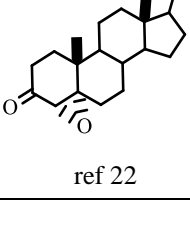
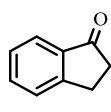
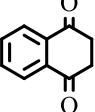
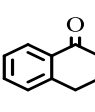
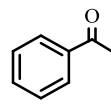
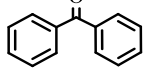
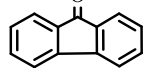
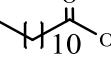
### General Procedure for [Ru<sup>III</sup>(Por)(Ph)(L)]-Catalyzed Epoxidation and C-H Oxidation

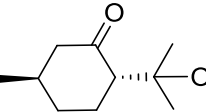
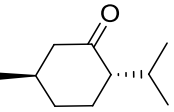
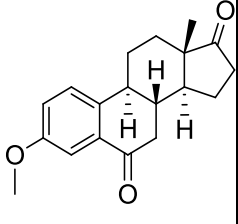
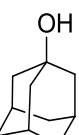
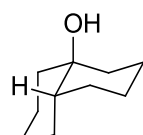
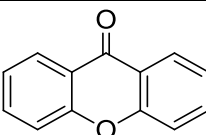
Catalyst [Ru<sup>III</sup>(Por)(Ph)(L)] (2 mol %) and *m*-CPBA/*n*-tetrabutylammonium periodate (0.167-0.525 mmol, depending on the substrate) were added to a Schlenk flask, which was then dried under vacuum and subsequently refilled with argon for three times. Under argon, alkene (0.150-0.167 mmol) was added before addition of freshly distilled CH<sub>2</sub>Cl<sub>2</sub> (2 mL). The reaction was stirred at room temperature (different reaction times, depending on the substrate). After the completion of reaction, the reaction mixture was evaporated to dryness and re-dissolved with 50 mL of diethyl ether/hexane or ethyl acetate/hexane (1:1 v/v) to remove most of the salt and catalyst. The filtered solution was then concentrated to give the crude product. If necessary, column chromatography was used to further purify the product with ethyl acetate/hexane as an eluent. The following table presents different internal

standards used to avoid peak overlap(s) in the determination of yield.

Internal Standard	Entries in Table 2
Dimethyl fumarate	9, 14, 16-18
2-Benzylpyridine	3, 10, 7, 11, 15
Methyl 4-nitrobenzene	2, 4-7

### References for Characterization of Organic Products

				
ref 10	ref 11	ref 12	ref 11	ref 13
				
ref 10	ref 14	ref 10	ref 15	ref 16
				
ref 10	ref 17	ref 17	ref 18	ref 19
				
ref 20	ref 16	ref 21	ref 21	ref 22
				
ref 22	ref 23	ref 24	ref 25	ref 26
				
ref 26	ref 27	ref 28	ref 29	ref 30

### Hammett Plot

In a typical run, ethylbenzene and *para*-substituted ethylbenzene (e.g. CH<sub>3</sub>, Cl, Br, NO<sub>2</sub>) in equimolar amounts (0.07 mmol each) were added to a Schlenk tube containing 2 mol % of **1** (0.0028 mmol) in CH<sub>2</sub>Cl<sub>2</sub> (2 mL). Upon well-mixing, 3.5 equiv of *m*-CPBA was charged to the tube. After 10 s, an aliquot (50  $\mu$ L) was quickly diluted by 20 times with CH<sub>2</sub>Cl<sub>2</sub>, and approximately 4  $\mu$ L of the diluted sample was immediately injected to GC-MS for detecting the ratio of acetophenones (the sampling time was determined by checking the % conversion of 4-ethyltoluene after 10 s, ensuring that % conversion was <5% and the reaction kinetics followed a pseudo-first-order rate law).

### Kinetic Measurements

In a UV cell, 10  $\mu$ M of **1** (3 mL of CH<sub>2</sub>Cl<sub>2</sub>) was added with 3 mM of *m*-CPBA (10  $\mu$ L of CH<sub>2</sub>Cl<sub>2</sub>, 1 equiv to **1**) to generate the Ru<sup>V</sup>-oxo species *in situ*. When the decrease in absorbance at 420 nm was stopped (formation of Ru<sup>V</sup>-oxo was accomplished), 10  $\mu$ L of ethylbenzene was added to the mixture. Addition of ethylbenzene made the absorbance at 420 nm to increase as the Ru<sup>V</sup>-oxo species was being reduced. In a similar manner, different amounts of ethylbenzene were added to the replicates containing **1** and *m*-CPBA. The different observed rate constants ( $k_{\text{obs}}$ ) were obtained by plotting ln|A-A<sub>∞</sub>| vs time (Figure S6–S15). After that, plotting  $k_{\text{obs}}$  vs concentration of ethylbenzene gave the second-order rate constant ( $k_2$ ). The same method was applied to the other liquid substrates. For some solid substrates, they were first dissolved in CH<sub>2</sub>Cl<sub>2</sub> to give stock solutions with known concentrations before adding to the *in situ* generated Ru<sup>V</sup>-oxo species.

### X-Band EPR Spectroscopy

In a vacuum-dried EPR tube, 0.6 mM of **1** in 500  $\mu$ L CH<sub>2</sub>Cl<sub>2</sub> was added and then immersed into liquid nitrogen. After 10 s, the frozen solution was cooled to 7 K by liquid helium, followed by recording its EPR

spectrum. When the measurement was finished, the solution was allowed to warm to room temperature and 1.2 equiv of *m*-CPBA was subsequently added. Similarly, the solution was again frozen by liquid nitrogen and cooled to 7 K by liquid helium. The EPR spectrum of this solution was then recorded. In a similar manner, the solution was warmed to room temperature and added with 4 equiv of styrene. After that, this solution was also frozen to record its EPR spectrum. In addition, the respective background EPR spectra were also obtained by recording the EPR spectra of CH<sub>2</sub>Cl<sub>2</sub>, *m*-CPBA in CH<sub>2</sub>Cl<sub>2</sub> and styrene in CH<sub>2</sub>Cl<sub>2</sub>.

### ESI-MS

Complex **1** (0.5 mM, 50 µL) was diluted by 125 times first and 250 µL of the diluted sample was then analyzed by ESI-MS. The ESI-MS spectrum was recorded at a flow rate of 5 µL/min, using positive-ion mode and spray voltage = 4.5 kV. After recording the ESI-MS spectrum, the residual solution was completely injected into a vial containing 0.9 equiv of *m*-CPBA, followed by analysis of the mixture immediately and continuously over 1.5 min. The solution was again injected back to a new vial containing 10 µL of styrene. The mixture was then analyzed by ESI-MS.

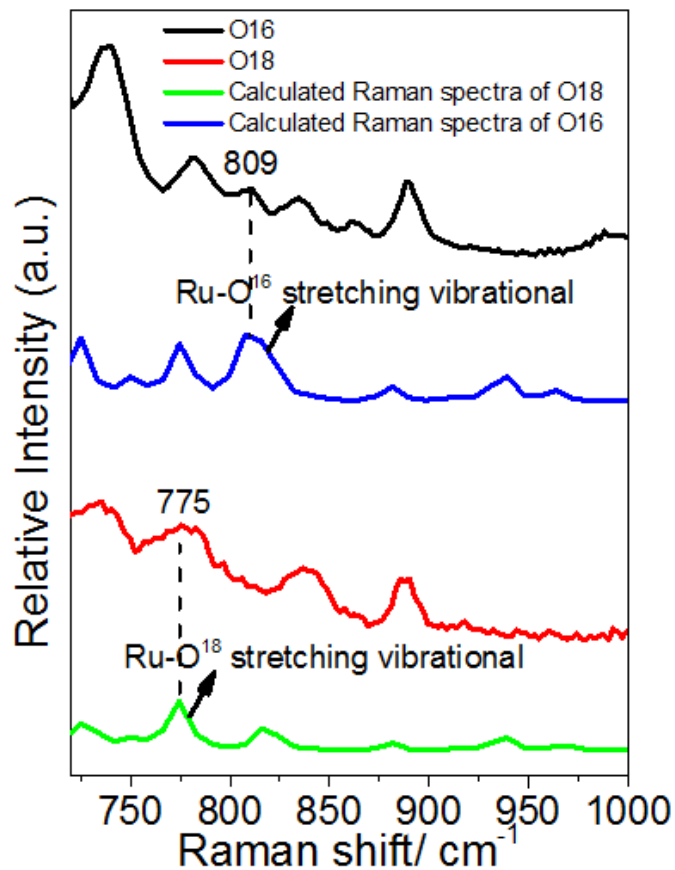
### Preparation of <sup>18</sup>O-Labeled *m*-CPBA

A small vial containing 2% H<sub>2</sub><sup>18</sup>O<sub>2</sub>(0.58 mmol) was placed in a 20-mL vial with CaH<sub>2</sub> (4.5 g). The H<sub>2</sub><sup>18</sup>O<sub>2</sub> solution was concentrated to 30-40% according to the total volume. After that, the H<sub>2</sub><sup>18</sup>O<sub>2</sub> solution was transferred to a 5-mL round-bottom flask using 2 mL of anhydrous 1,4-dioxane, followed by addition of NaOH (0.58 mmol). The reaction mixture was sonicated for 3 min until turbidity appeared. The flask was charged with a small amount of anhydrous MgSO<sub>4</sub> (0.01 mmol) and cooled to 0 °C. 3-Chlorobenzoyl chloride was injected to the reaction mixture under surface and allowed to stir for 30 min at 0 °C. After that, cold 20% H<sub>2</sub>SO<sub>4</sub> was used to acidify the reaction mixture. The organic phase was extracted with CH<sub>2</sub>Cl<sub>2</sub> and the combined organic phase was back extracted with water. A flaky white solid was obtained after removal of organic solvent under vacuum at room temperature (50 mg, 50% yield; when the solid was added to a solution of **1**, the pattern of UV-vis spectral change was the same as that obtained by treating **1** with *m*-CPBA-<sup>16</sup>O). The solid was used for resonance Raman spectroscopy without further purification.

### Resonance Raman (RR) Spectroscopy

The RR experiments were done by employing an experimental setup and methods detailed previously<sup>37</sup> and only a brief description is provided here. RR spectra were measured using 416 nm excitation wavelength which is the first Stokes hydrogen Raman-shifted laser line produced from the third harmonic of Nd:YAG laser. The power of 416 nm is about 5 mW. The samples were dissolved in CH<sub>2</sub>Cl<sub>2</sub> and MeCN solvents with an absorbance of ~1 at 416 nm in a 2 mm path-length fused silica cuvette throughout the data acquisition. The excitation laser beam was focused to about a 0.5 mm diameter spot size onto a 2 mm path-length

cuvette of sample. A backscattering geometry was employed for sample excitation and for collection of the Raman scattered light by reflective optics. The Raman signal detected by a liquid-nitrogen-cooled charged-coupled device (CCD) detector was acquired for 10 s before being read out to an interfaced personal computer, and 6 of these readouts were averaged to obtain the resonance Raman spectrum. The Raman bands of the MeCN solvent were employed to calibrate the resonance Raman spectra with an estimated accuracy of  $5\text{ cm}^{-1}$  in absolute frequency. The Raman spectrum of the sample was obtained by removing the Raman spectrum of the corresponding solvent with a proper scaling factor. For the sampling procedure, 1 mM of **1** in  $\text{CH}_2\text{Cl}_2$  was used to record an initial spectrum. 1.2 equiv of  $^{16}\text{O}$ -labeled *m*-CPBA was then added to the solution that was just recorded, followed by recording another spectrum. In a similar manner,  $^{18}\text{O}$ -labeled *m*-CPBA was added to a replicate solution containing 1 mM of **1**. Due to limited solubility of **1** in MeCN, only 0.1 mM solution of **1** in MeCN was used to record the initial spectrum. After recording the initial spectrum, two spectra were also separately recorded in the presence of 10  $\mu\text{L}$   $\text{H}_2^{16}\text{O}$  and  $\text{H}_2^{18}\text{O}$  (97% atom  $^{18}\text{O}$ ).



Simulated and experimental RR spectra for oxidation of **1** by *m*-CPBA.

## Computational Details

All calculations were performed through Gaussian 09 package.<sup>38</sup> All the structures were optimized at the M11L/MG3S/M11L/def2-SVP<sup>39</sup> level of density functional theory (DFT). The separated reactants were used as the zero reference. Vibrational analysis was performed for all the stationary points to characterize the transition state (one imaginary frequency), the corresponding reactant complex (no imaginary frequency), and product complex (no imaginary frequency). To further refine the energies, the solvent effect was included by the single point calculations for all the optimized gas-phase structures with self-consistent reactions field (SCRF) based on the SMD continuum solvation model<sup>40</sup> in which dichloromethane was the solvent as the experimental condition. The functional of M06 still was applied; time-dependent density functional theory (TD-DFT) calculation was carried out using B3LYP-GD3BJ/def2-SVP.<sup>41</sup>

The EPR *g*-tensors of [Ru<sup>III</sup>(TDCPP)(Ph)] and [Ru<sup>V</sup>(TDCPP)(O)(Ph)] were calculated using a literature method.<sup>42</sup> The calculations were performed by employing the ORCA program<sup>43</sup> at the level of theory BP86/def2-TZVP<sup>44</sup> based on the optimized structures obtained by Gaussian 09 package.

The KIE was calculated with the transition state theory rate constants including one-dimensional tunneling effect (TSTW) by the Kinetic and Statistical Thermodynamical Package.<sup>45</sup> The Wigner tunneling corrected rate constant  $k_{TSTW}$  is defined as follows:

$$k_{TSTW} = \chi(T) \cdot \left[ \sigma \times \frac{k_b T}{h} \times \left( \frac{RT}{P^0} \right)^{\Delta n} \times e^{-\Delta G^{\ddagger 0} / k_b T} \right]$$

wherein  $\chi(T)$  is the transmission coefficient, which is defined as

$$\chi(T) = 1 + \frac{h^2 |v^\ddagger|^2 \beta^2}{24}$$

The UV-vis spectra of [Ru<sup>V</sup>(TDCPP)(O)(Ph)] (<sup>2</sup>A<sub>1</sub>), [Ru<sup>VI</sup>(TDCPP)(O)<sub>2</sub>], and [Ru<sup>III</sup>(TDCPP)(Ph)] were calculated through TD-DFT. As shown in the following table, the calculated Soret band of [Ru<sup>V</sup>(TDCPP)(O)(Ph)] is red-shifted relative to that of [Ru<sup>III</sup>(TDCPP)(Ph)], which is consistent with the experimental observations (see Figure 3 in text).

Calculated and Experimental  $\lambda_{\max}$  ( $\log \epsilon$ ) Values for Soret Bands

	Calc $\lambda_{\max}$ /nm ( $\log \epsilon$ )	Expt $\lambda_{\max}$ /nm ( $\log \epsilon$ )
[Ru <sup>VI</sup> (TDCPP)(O) <sub>2</sub> ]	397 (5.46)	420 (5.42) <sup>a</sup>
[Ru <sup>III</sup> (TDCPP)(Ph)]	386 (5.09)	405 (5.10)
[Ru <sup>V</sup> (TDCPP)(O)(Ph)]	413 (4.66)	416 ( <sup>b</sup> )

<sup>a</sup> Data from Liu, C.-J.; Yu, W.-Y.; Che, C.-M.; Yeung, C.-H. *J. Org. Chem.* **1999**, *64*, 7365. <sup>b</sup> Not available.

## References

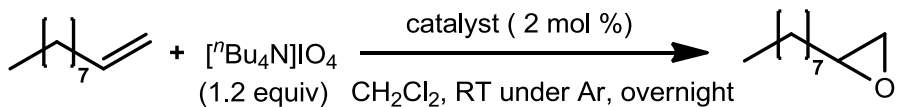
- (1) Dauban, P.; Sanière, L.; Tarrade, A.; Dodd, R. H. *J. Am. Chem. Soc.* **2001**, *123*, 7707.
- (2) (a) Johnstone, R. A. W.; Nunes, L. P. G.; Pereira, M. M.; Rocha Gonsalves, A. M. d'A.; Serra, A. C. *Heterocycles* **1996**, *43*, 1423. (b) Lv, H.; Yang, B.; Jing, J.; Yu, Y.; Zhang, J.; Zhang, J.-L. *Dalton Trans.* **2012**, *41*, 3116.
- (3) Wei, X.-J.; Yang, D.-T.; Wang, L.; Song, T.; Wu, L.-Z.; Liu, Q. *Org. Lett.* **2013**, *15*, 6054.
- (4) Tseng, C. C.; Paisley, S. D.; Goering, H. L. *J. Org. Chem.* **1986**, *51*, 2884.
- (5) Hu, W.-X.; Li, P.-R.; Jiang, G.; Che, C.-M.; Chen, J. *Adv. Synth. Catal.* **2010**, *352*, 3190.
- (6) Takagi, S.; Miyamoto, T. K.; Hamaguchi, M.; Sasaki, Y. *Inorg. Chim. Acta* **1990**, *173*, 215.
- (7) Proteum2, *Bruker AXS, Madison, Wisconsin*, **1999**.
- (8) Sheldrick, G. *Acta Crystallogr. Section A* **2008**, *64*, 112.
- (9) Dolomanov, O. V.; Bourhis, L. J.; Gildea, R. J.; Howard, J. A. K.; Puschmann, H. *J. Appl. Crystallogr.* **2009**, *42*, 339.
- (10) Piccinini, A.; Kavanagh, S. A.; Connon, P. B.; Connon, S. J. *Org. Lett.* **2010**, *12*, 608.
- (11) Tse, M. K.; Bhor, S.; Klawonn, M.; Anikumar, G.; Jiao, H.; Spannenberg, A.; Döbler, C.; Mägerlein, W.; Hugl, H.; Beller, M. *Chem.-Eur. J.* **2006**, *12*, 1875.
- (12) Pedragosa-Moreau, S.; Morisseau, C.; Zylber, J.; Archelas, A.; Baratti, J.; Furstoss, R. *J. Org. Chem.* **1996**, *61*, 7402.
- (13) Imada, Y.; Iida, H.; Kitagawa, T.; Naota, T. *Chem.-Eur. J.* **2011**, *17*, 5908.
- (14) Matsumoto, K.; Kubo, T.; Katsuki, T. *Chem.-Eur. J.* **2009**, *15*, 6573.
- (15) Susanto, W.; Lam, Y. *Tetrahedron* **2011**, *67*, 8353.
- (16) Schomaker, J. M.; Reddy Pulgam, V.; Borhan, B. *J. Am. Chem. Soc.* **2004**, *126*, 13600.
- (17) Brimeyer, M. O.; Mehrota, A.; Quici, S.; Nigam, A.; Regen, S. L. *J. Org. Chem.* **1980**, *45*, 4254.
- (18) Murphy, A.; Pace, A.; Stack, T. D. P. *Org. Lett.* **2004**, *6*, 3119.
- (19) Arai, K.; Lucarini, S.; Salter, M. M.; Ohta, K.; Yamashita, Y.; Kobayashi, S. *J. Am. Chem. Soc.* **2007**, *129*, 8103.
- (20) Li, Y.; Liu, X.; Yang, Y.; Zhao, G. *J. Org. Chem.* **2007**, *72*, 288.
- (21) Chan, W.-K.; Wong, M.-K.; Che, C.-M. *J. Org. Chem.* **2005**, *70*, 4226.
- (22) Labra-Vázquez, P.; Galano, A.; Romero-Ávila, M.; Flores-Álamo, M.; Iglesias-Arteaga, M. A.; ARKIVOC **2013**, *4*, 107.
- (23) Kumar, R. A.; Maheswari, C. U.; Ghantasala, S.; Jyothi, C.; Reddy, K. R. *Adv. Synth. Catal.* **2011**, *353*, 401.
- (24) Metallinos, C.; Zaifman, J.; Belle, L. V.; Dodge, L.; Pilkington, M. *Organometallics* **2009**, *28*, 4534.
- (25) Cunningham, A.; Mokal-Parekh, V.; Wilson, C.; Woodward, S. *Org. Biomol. Chem.* **2004**, *2*, 741.
- (26) Yuan, Y.; Shi, X. *Synlett* **2011**, *4*, 559.
- (27) Thirunavukkarasu, V. S.; Parthasarathy, K.; Cheng, C.-H. *Angew. Chem., Int. Ed.* **2008**, *47*, 9462.
- (28) van E. Hommes, N. J. R.; Clark, T. *J. Mol. Model.* **2005**, *11*, 175.
- (29) Russ, A. S.; Vinken, R.; Schuphan, I.; Schmidt, B. *Chemosphere* **2005**, *60*, 1624.
- (30) Rani, S.; Khan, S. A.; Ali, M. *Nat. Prod. Res.* **2010**, *24*, 1358.
- (31) Molander, G. A.; Hahn, G. *J. Org. Chem.* **1986**, *51*, 2596.
- (32) Dohi, T.; Maruyama, A.; Yoshimura, M.; Morimoto, K.; Tohma, H.; Shiro, M.; Kita, Y. *Chem. Commun.* **2005**, 2205.
- (33) Iida, T.; Ogawa, S.; Miyata, S.; Goto, T.; Mano, N.; Goto, J.; Nambara, T. *Lipids* **2004**, *39*, 873-880.
- (34) Brodsky, B. H.; Du Bois, J. *J. Am. Chem. Soc.* **2005**, *127*, 15391.
- (35) Kamata, K.; Yonehara, K.; Nakagawa, Y.; Uehara, K.; Mizuno, N. *Nature Chem.* **2010**, *2*, 478.
- (36) Zhao, J.; Larock, R. C. *Org. Lett.* **2005**, *7*, 4273.
- (37) (a) Chan, P. Y.; Kwok, W. M.; Lam, S. K.; Chiu, P.; Phillips, D. L. *J. Am. Chem. Soc.* **2005**, *127*, 8246. (b) Li, M. D.; Yeung, C. S.; Guan, X.; Ma, J.; Li, W.; Ma, C.; Phillips, D. L. *Chem.-Eur. J.* **2011**, *17*, 10935.
- (38) Frisch, M. J.; Trucks, G. W.; Schlegel, H. B.; Scuseria, G. E.; Robb, M. A.; Cheeseman, J. R.; Scalmani, G.; Barone, V.; Mennucci, B.; Petersson, G. A.; Nakatsuji, H.; Caricato, M.; Li, X.; Hratchian, H. P.; Izmaylov, A. F.; Bloino, J.; Zheng, G.; Sonnenberg, J. L.; Hada, M.; Ehara, M.; Toyota, K.; Fukuda, R.; Hasegawa, J.; Ishida, M.; Nakajima, T.; Honda, Y.; Kitao, O.; Nakai, H.; Vreven, T.; Montgomery, J. A.; Peralta, J. E.; Ogliaro, F.; Bearpark, M.; Heyd, J. J.; Brothers, E.; Kudin, K. N.; Staroverov, V. N.; Kobayashi, R.; Normand, J.; Raghavachari, K.; Rendell, A.; Burant, J. C.; Iyengar, S. S.; Tomasi, J.; Cossi, M.; Rega, N.; Millam, J. M.; Klene, M.; Knox, J.

- E.; Cross, J. B.; Bakken, V.; Adamo, C.; Jaramillo, J.; Gomperts, R.; Stratmann, R. E.; Yazyev, O.; Austin, A. J.; Cammi, R.; Pomelli, C.; Ochterski, J. W.; Martin, R. L.; Morokuma, K.; Zakrzewski, V. G.; Voth, G. A.; Salvador, P.; Dannenberg, J. J.; Dapprich, S.; Daniels, A. D.; Farkas; Foresman, J. B.; Ortiz, J. V.; Cioslowski, J.; Fox, D. J. *Gaussian 09*, revision C.01; Gaussian, Inc.: Wallingford, CT, 2011.
- (39) (a) Peverati, R.; Truhlar, D. G. *J. Phys. Chem. Lett.* **2012**, *3*, 117. (b) Zheng, J.; Xu, X.; Truhlar, D. G. *Theor. Chem. Acc.* **2011**, *128*, 295. (c) Weigend, F.; Ahlrichs, R. *Phys. Chem. Chem. Phys.* **2005**, *7*, 3297.
- (40) Marenich, A. V.; Cramer, C. J.; Truhlar, D. G. *J. Phys. Chem. B* **2009**, *113*, 6378.
- (41) (a) Becke, A. D. *Phys. Rev. A* **1988**, *38*, 3098. (b) Lee, C.; Yang, W.; Parr, R. G. *Phys. Rev. B* **1988**, *37*, 785. (c) Grimme, S.; Antony, J.; Ehrlich, S.; Krieg, H. *J. Chem. Phys.* **2010**, *132*, 154104. (d) Grimme, S.; Ehrlich, S.; Goerigk, L. *J. Comput. Chem.* **2011**, *32*, 1456.
- (42) Scheibel, M. G.; Askevold, B.; Heinemann, F. W.; Reijerse, E. J.; de Bruin, B.; Schneider, S. *Nature Chem.* **2012**, *4*, 552.
- (43) Neese, F. *WIREs Comput. Mol. Sci.*, **2012**, *2*, 73.
- (44) (a) Perdew, J. P. *Phys. Rev. B* **1986**, *33*, 8822. (b) Becke, A. D. *Phys. Rev. A* **1988**, *38*, 3098.
- (45) Canneaux, S.; Bohr, F.; Henon, E. *J. Comput. Chem.* **2014**, *35*, 82.

**Table S1. Crystallographic Data for Complexes 1–3.**

complex	<b>1</b>	<b>2</b>	<b>3</b>
Chemical formula	C <sub>54</sub> H <sub>35</sub> Cl <sub>8</sub> N <sub>4</sub> ORu C <sub>4</sub> H <sub>10</sub> O · 0.5C <sub>6</sub> H <sub>14</sub>	C <sub>50</sub> H <sub>27</sub> F <sub>8</sub> N <sub>4</sub> ORu · H <sub>2</sub> O	C <sub>48</sub> H <sub>28</sub> ClF <sub>8</sub> N <sub>4</sub> ORu · 0.5C <sub>4</sub> H <sub>8</sub> O
crystal system	Monoclinic	Monoclinic	Orthorhombic
space group	P2 <sub>1</sub> /n	C2/c	P2 <sub>1</sub> 2 <sub>1</sub> 2 <sub>1</sub>
temperature (K)	100	100	100
<i>a</i> (Å)	12.5729(12)	20.0727(13)	11.4235(5)
<i>b</i> (Å)	21.6205(16)	12.7833(8)	20.7153(9)
<i>c</i> (Å)	21.910(2)	20.2135(13)	39.4855(17)
β (°)	95.011(4)	109.0865(17)	90
<i>V</i> (Å <sup>3</sup> )	5932.9(9)	4901.6(5)	9343.9(7)
<i>Z</i>	4	4	8
radiation type	Cu <i>K</i> α	Cu <i>K</i> α	Cu <i>K</i> α
μ (mm <sup>-1</sup> )	5.81	3.21	3.89
crystal size (mm)	0.25 × 0.06 × 0.06	0.3 × 0.2 × 0.03	0.25 × 0.25 × 0.15
(sin θ/λ) <sub>max</sub> (Å <sup>-1</sup> )	0.597	0.599	0.597
no. of reflections	10195	4289	16366
no. of parameters	707	332	1157
no. of restraints	18	93	93
<i>R</i> [ <i>F</i> <sup>2</sup> > 2σ( <i>F</i> <sup>2</sup> )]	0.064	0.057	0.057
<i>wR</i> ( <i>F</i> <sup>2</sup> )	0.178	0.160	0.177
<i>S</i>	1.07	1.13	1.13
Δρ <sub>max</sub> , Δρ <sub>min</sub> (eÅ <sup>-3</sup> )	1.56, -1.29	1.44, -0.44	1.20, -0.46

**Table S2. Catalyst Screening for the Oxidation of 1-Decene with  $[^n\text{Bu}_4\text{N}]\text{IO}_4$ .<sup>a</sup>**



entry	catalyst	yield (%) <sup>b</sup>
1	none	no reaction
2	$[\text{Ru}^{\text{II}}(\text{TDCPP})(\text{CO})]$	no reaction
3	$[\text{Ru}^{\text{III}}(\text{TDCPP})(\text{Ph})(\text{OEt}_2)]$	75% <sup>c</sup>
4	$[\text{Ru}^{\text{IV}}(\text{TDCPP})(\text{Cl})_2]$	Trace
5	$[\text{Ru}^{\text{VI}}(\text{TDCPP})(\text{O})_2]$	no reaction <sup>d</sup>
6	$[\text{Ru}^{\text{VI}}(\text{TDCPP})(\text{O})_2]$	3% <sup>e</sup>
7	$[\text{Ru}^{\text{III}}(\text{TDFPP})(\text{Cl})(\text{THF})]$	no reaction

<sup>a</sup> Reaction conditions: catalyst (3.34  $\mu\text{mol}$ ), 1-decene (0.167 mmol) and oxidant (0.200 mmol) in  $\text{CH}_2\text{Cl}_2$  (5 mL), RT, Ar atmosphere. <sup>b</sup>  $^1\text{H}$  NMR yield:  $[\text{epoxide}] / \{ [\text{alkene}] + [\text{epoxide}] \} \times 100\%$ . <sup>c</sup> 1.5 mol % of **1**. <sup>d</sup> 6 h. <sup>e</sup> 40 °C.

**Table S3. Data Used to Plot the Hammett Correlation for 1-Catalyzed C-H Oxidation of *para*-Substituted Ethylbenzenes with *m*-CPBA.**

<i>p</i> -X-C <sub>6</sub> H <sub>4</sub> Et	X				
	Me	H	Cl	Br	NO <sub>2</sub>
Product areas A <sub>X</sub> :A <sub>H</sub> <sup>a</sup>	19334:5720	N/A	11747:18563	12638:25645	822:13714
<i>k</i> <sub>rel</sub>	3.4	1	0.63	0.49	0.06
log( <i>k</i> <sub>rel</sub> )	0.53	0	-0.20	-0.31	-1.22
$\sigma^+$ <sup>b</sup>	-0.311	0	+0.114	+0.150	+0.790

<sup>a</sup> A<sub>X</sub>: product area from *para*-substituted ethylbenzene; A<sub>H</sub>: product area from ethylbenzene.

<sup>b</sup> Values taken from: Brown, H. C.; Okamoto, Y. *J. Am. Chem. Soc.* **1958**, *80*, 4979.

**Table S4. Rate Constants ( $k_2$ ) for the Oxidation of Hydrocarbons by ‘1 + *m*-CPBA (1 equiv)’.**

Substrate	$k_2$ (M <sup>-1</sup> s <sup>-1</sup> )	Substrate	$k_2$ (M <sup>-1</sup> s <sup>-1</sup> )
Methylcyclohexane	0.220±0.006	Methylcyclohexane- <i>d</i> <sub>14</sub>	0.050±0.003
1-Phenylethanol	2.48±0.08	1-Phenylethanol- <i>d</i> <sub>10</sub>	0.78±0.02
Ethylbenzene	1.99±0.04	1-Decene	15.34±0.73
Xanthene	33.62±0.39		
Fluorene	9.33±0.09		
9,10-Dihydroanthracene (DHA)	33.82±0.09		

**Table S5. Comparison of the *g* Tensors for Examples of Ru Species with *S* = 1/2.**

Ru species with <i>S</i> = 1/2	<i>g</i> tensor			$g_{\text{iso}} = (g_x + g_y + g_z)/3$
	$g_x$	$g_y$	$g_z$	
[Ru <sup>V</sup> (TDCPP)(O)(Ph)] (experimental; this work)	2.038	1.983	1.890	1.970
[Ru <sup>V</sup> (TDCPP)(O)(Ph)] (calculated; this work)	2.042	2.015	1.946	2.001
[ <sup>7</sup> Pr <sub>4</sub> N][Ru <sup>V</sup> (O <sub>2</sub> COCEt <sub>2</sub> ) <sub>2</sub> (O)] <sup>a</sup> (experimental)	2.076	1.977	1.910	1.988
[Ru <sup>V</sup> (bda)(isoq) <sub>2</sub> (O)] <sup>b</sup> (experimental)	2.070	2.000	1.850-1.910	1.973-1.993
[Ru <sup>V</sup> (bpy) <sub>2</sub> (O)(OH)] <sup>2+</sup> <sup>c</sup> (experimental)	2.065	2.004	1.868	1.979
[Ru <sup>III</sup> (TDCPP)(Ph)] (calculated; this work)	2.831	2.253	2.037	2.374
[Ru <sup>III</sup> (F <sub>20</sub> -TPP)(OEt)] <sup>d</sup> (experimental)	2.53	2.12	1.89	2.18
[Ru <sup>III</sup> (F <sub>20</sub> -TPP)(OD)(X)] <sup>e</sup> (experimental)	2.55	2.55	2.05	2.38
[Ru <sup>III</sup> (OEP)(PPh <sub>3</sub> )(Br)] <sup>f</sup> (experimental)	2.31	2.31	1.98	2.20

<sup>a</sup> Ref: Dengel, A. C.; Griffith, W. P. *Inorg. Chem.* **1991**, *30*, 869.<sup>b</sup> bda = 2,2'-bipyridine-6,6'-dicarboxylate; isoq = isoquinoline;  $g_z$  obscured by the background signal of indium tin oxide; ref: Lebedev, D.; Pineda-Galvan, Y.; Tokimaru, Y.; Fedorov, A.; Kaeffer, N.; Copéret, C.; Pushkar, Y. *J. Am. Chem. Soc.* **2018**, *140*, 451.<sup>c</sup> bpy = 2,2'-bipyridine; ref: Planas, N.; Vigara, L.; Cady, C.; Miro, P.; Huang, P.; Hammarstrom, L.; Styring, S.; Leidel, N.; Dau, H.; Haumann, M.; Gagliardi, L.; Cramer, C. J.; Llobet, A. *Inorg. Chem.* **2011**, *50*, 11134.<sup>d</sup> Ref: Wang, C.; Shalyaev, K. V.; Bonchio, M.; Carofiglio, T.; Groves, J. T. *Inorg. Chem.* **2006**, *45*, 4769.<sup>e</sup> OD = oxygen donor; X = OD or other ligands;  $g_{\perp} = g_x = g_y = 2.550$ ,  $g_{\parallel} = g_z = 2.050$ ; ref: Groves, J. T.; Bonchio, M.; Carofiglio, T.; Shalyaev, K., *J. Am. Chem. Soc.* **1996**, *118*, 8961.<sup>f</sup>  $g_{\perp} = g_x = g_y = 2.31$ ,  $g_{\parallel} = g_z = 1.98$ ; ref: James, B. R.; Dolphin, D.; Leung, T. W.; Einstein, F. W. B.; Willis, A. C. *Can. J. Chem.* **1984**, *62*, 1238.

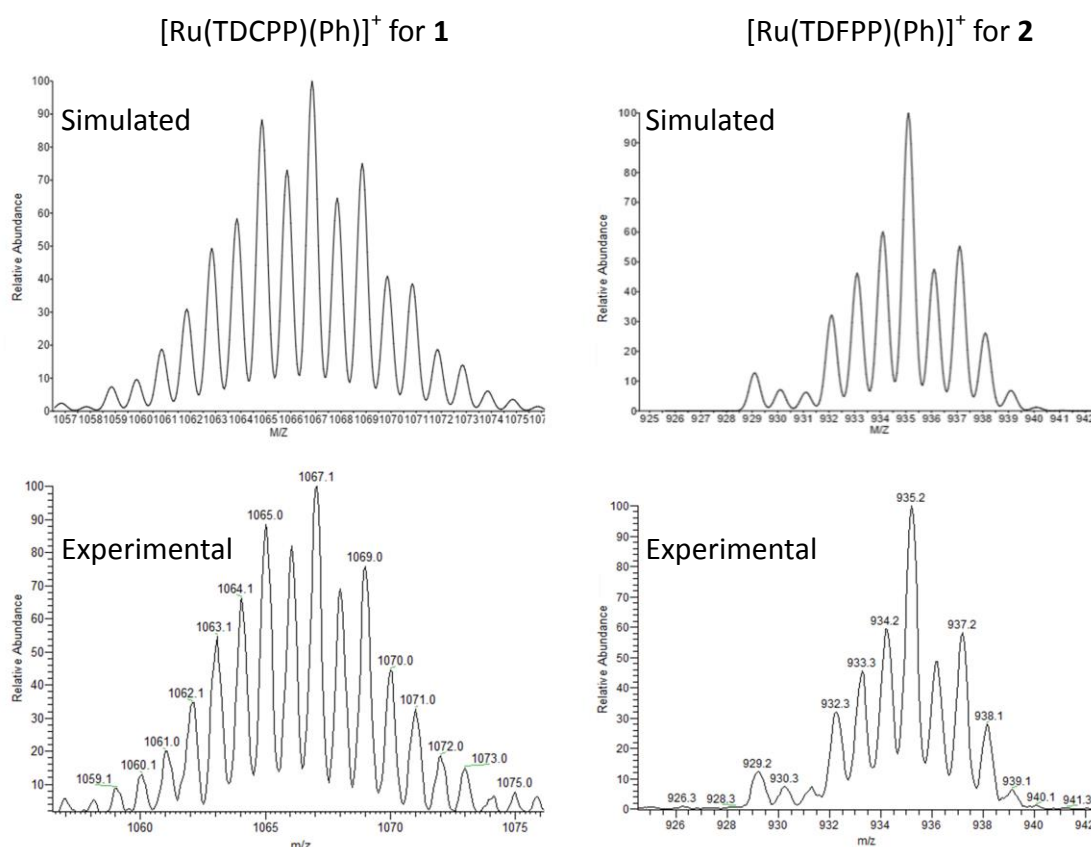


**Figure S1.** ESI-MS spectra of  $[\text{Ru}^{\text{III}}(\text{TDCPP})(\text{Ph})(\text{OEt}_2)]$  (**1**) and  $[\text{Ru}^{\text{III}}(\text{TDFPP})(\text{Ph})(\text{OH}_2)]$  (**2**): Simulated and experimental isotopic patterns for  $[\text{Ru}(\text{Por})(\text{Ph})]^+$ .

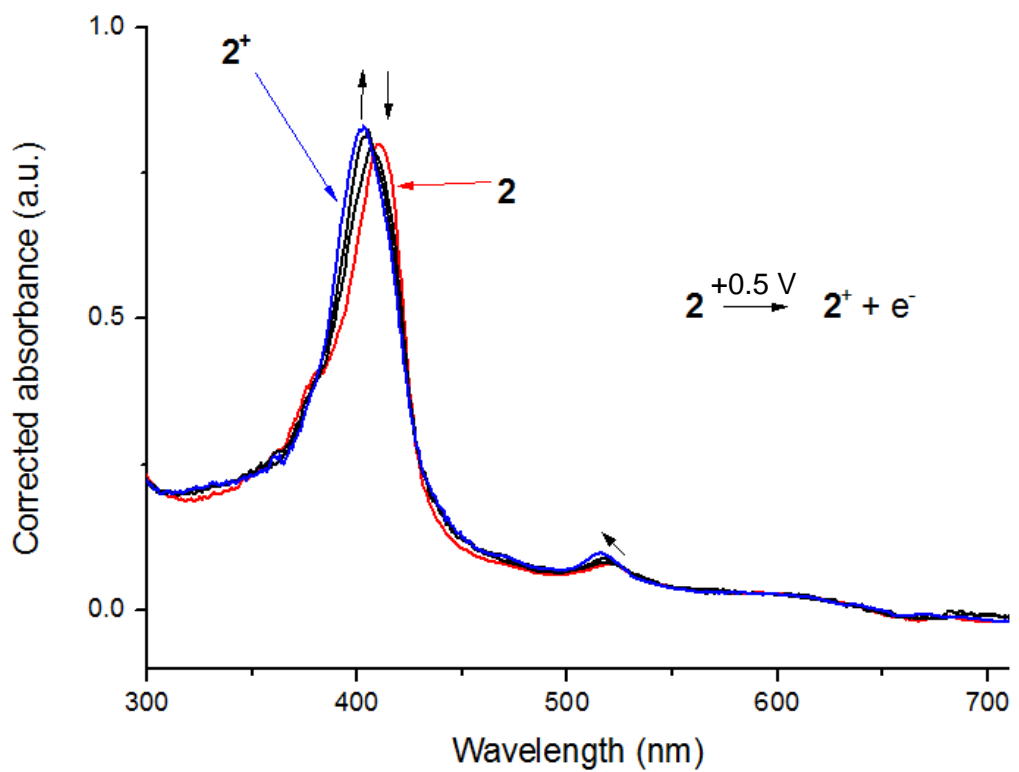


**Figure S2.** UV-vis spectral change of the electrochemical oxidation of **2** (20 s-intervals) at constant voltage (+0.5 V) in the presence of 0.1 M electrolyte ( $[{}^n\text{Bu}_4\text{N}]\text{PF}_6$ ).

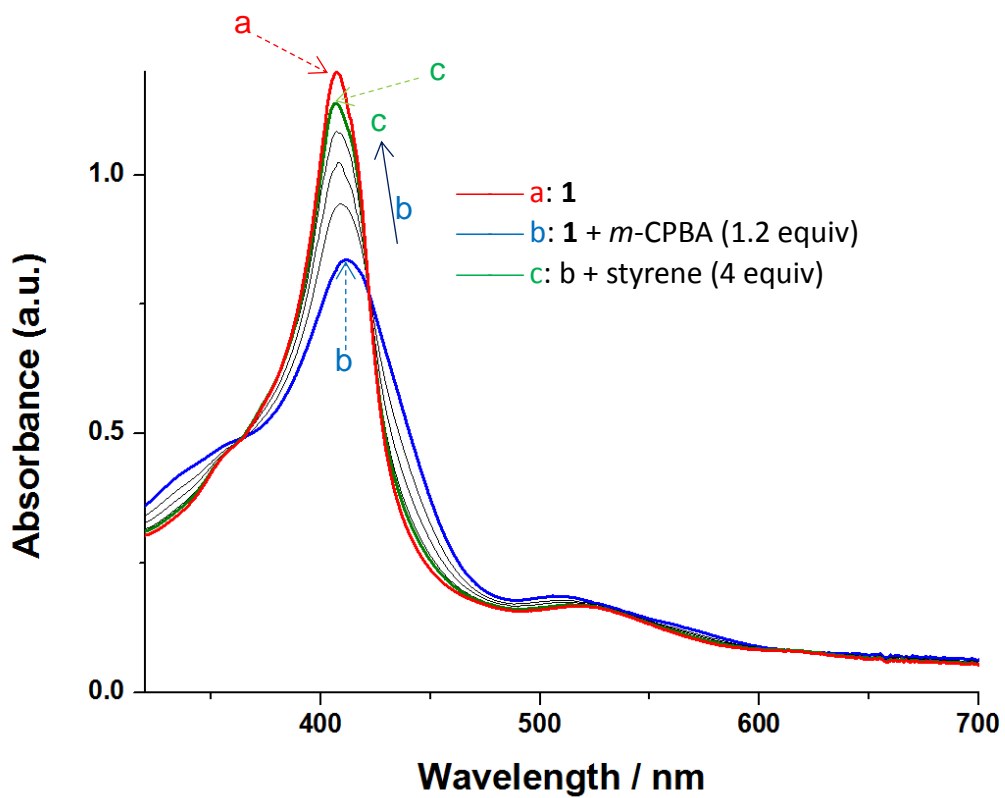


**Figure S3.** UV-vis spectral changes. Treatment of **1** with *m*-CPBA (1.2 equiv) in CH<sub>2</sub>Cl<sub>2</sub> at -35 °C immediately changed the spectrum from (a) to (b); subsequent treatment of (b) with styrene (4 equiv) changed the spectrum to (c) via black curves after 10 min.

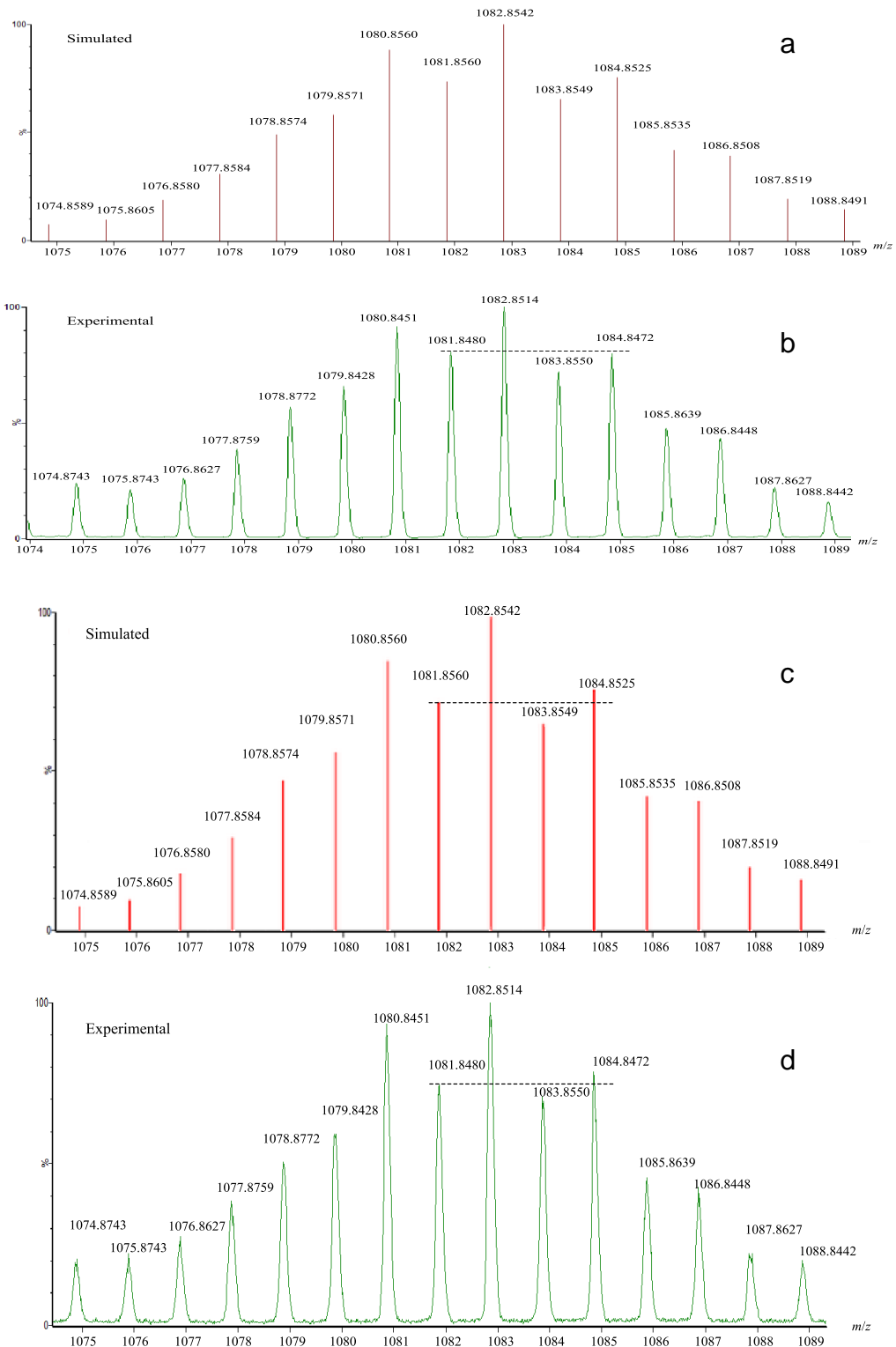


**Figure S4.** (a) Simulated and (b) observed isotopic pattern for the parent ion of  $[Ru(TDCPP)(O)(Ph)]$  (**A**). (c) Simulated isotope pattern for ‘95%  $[Ru(TDCPP)(Ph)^{16}O]$  + 5%  $[Ru(TDCPP)(Ph)^{18}O]$ ’. (d) Observed isotope pattern for the signal at  $m/z$  1082.8514 generated from reaction of **1** with *m*-CPBA in the presence of  $^{18}OH_2$ . Experimental details for (b): solvent  $CH_2Cl_2$ , **1** (0.2 mM, 230  $\mu$ L), *m*-CPBA (4.6 mM, 10  $\mu$ L; 1 equiv). Experimental details for (d): solvent  $CH_2Cl_2/MeCN$  (1:1), **1** (0.2 mM, 230  $\mu$ L), *m*-CPBA (4.6 mM, 10  $\mu$ L; 1 equiv),  $^{18}OH_2$  (10  $\mu$ L, large excess). Since the hydrophobic Ru-oxo species was neutral, water/oxo exchange could become sluggish/insignificant even if a polar mixed-solvent system was employed.

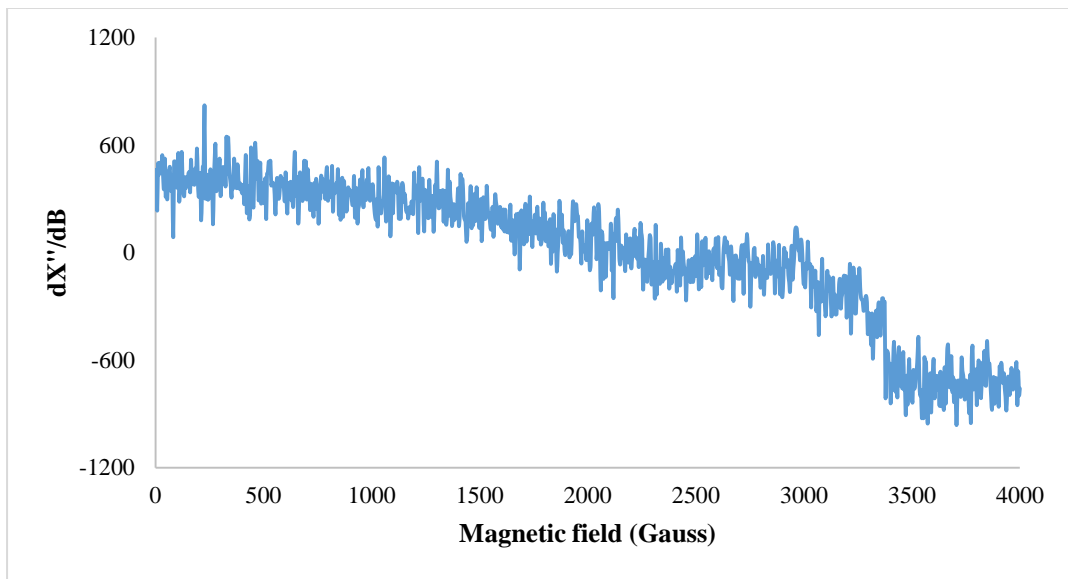


**Figure S5.** X-band EPR spectrum of **1** recorded at 40 K.

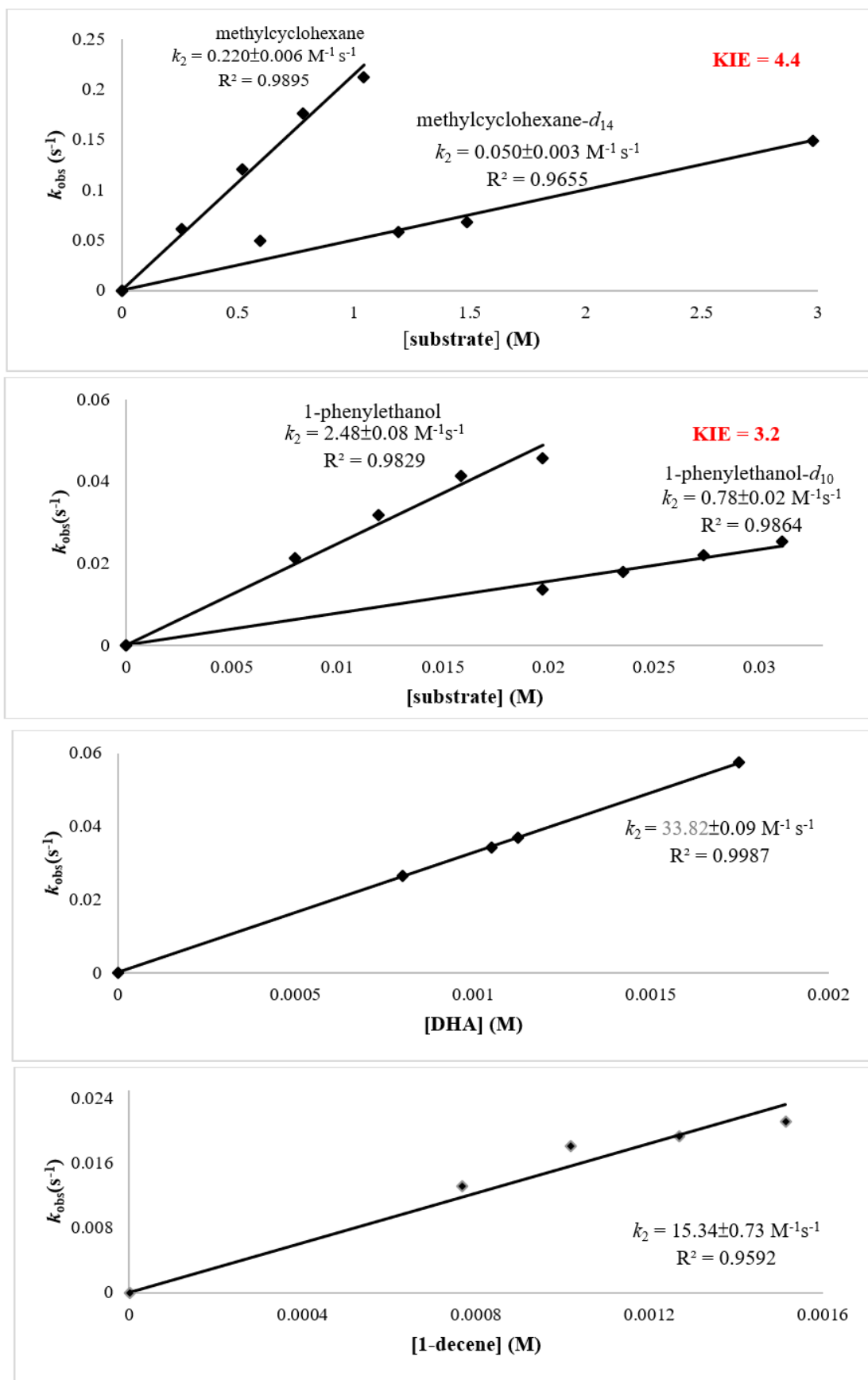


**Figure S6a.** Graphs showing  $k_{\text{obs}}$  of hydrocarbon oxidation by **1** vs concentration of hydrocarbons (298 K).

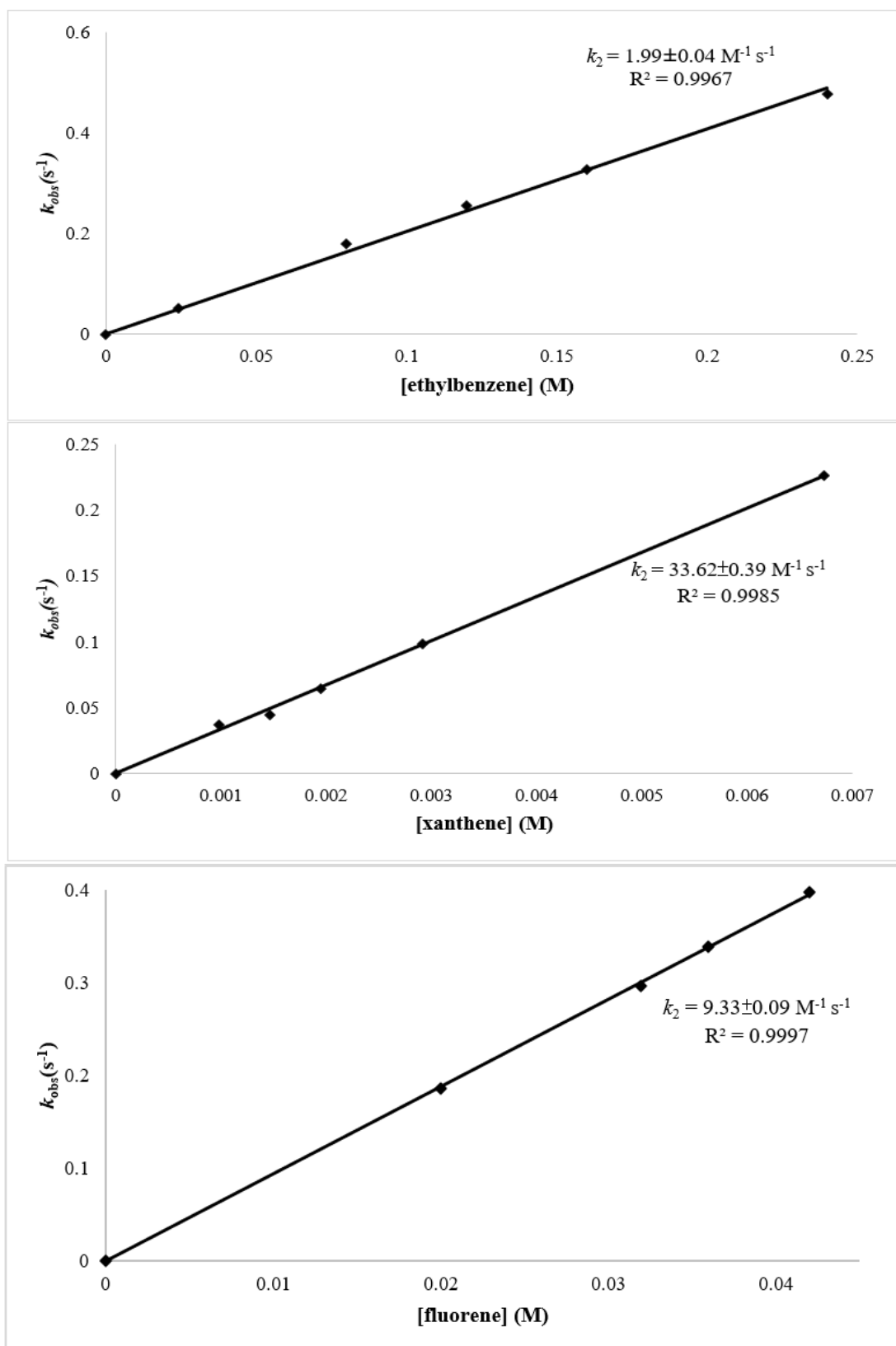


**Figure S6b.** Graphs showing  $k_{obs}$  of hydrocarbon oxidation by **1** vs concentration of hydrocarbons (298 K).

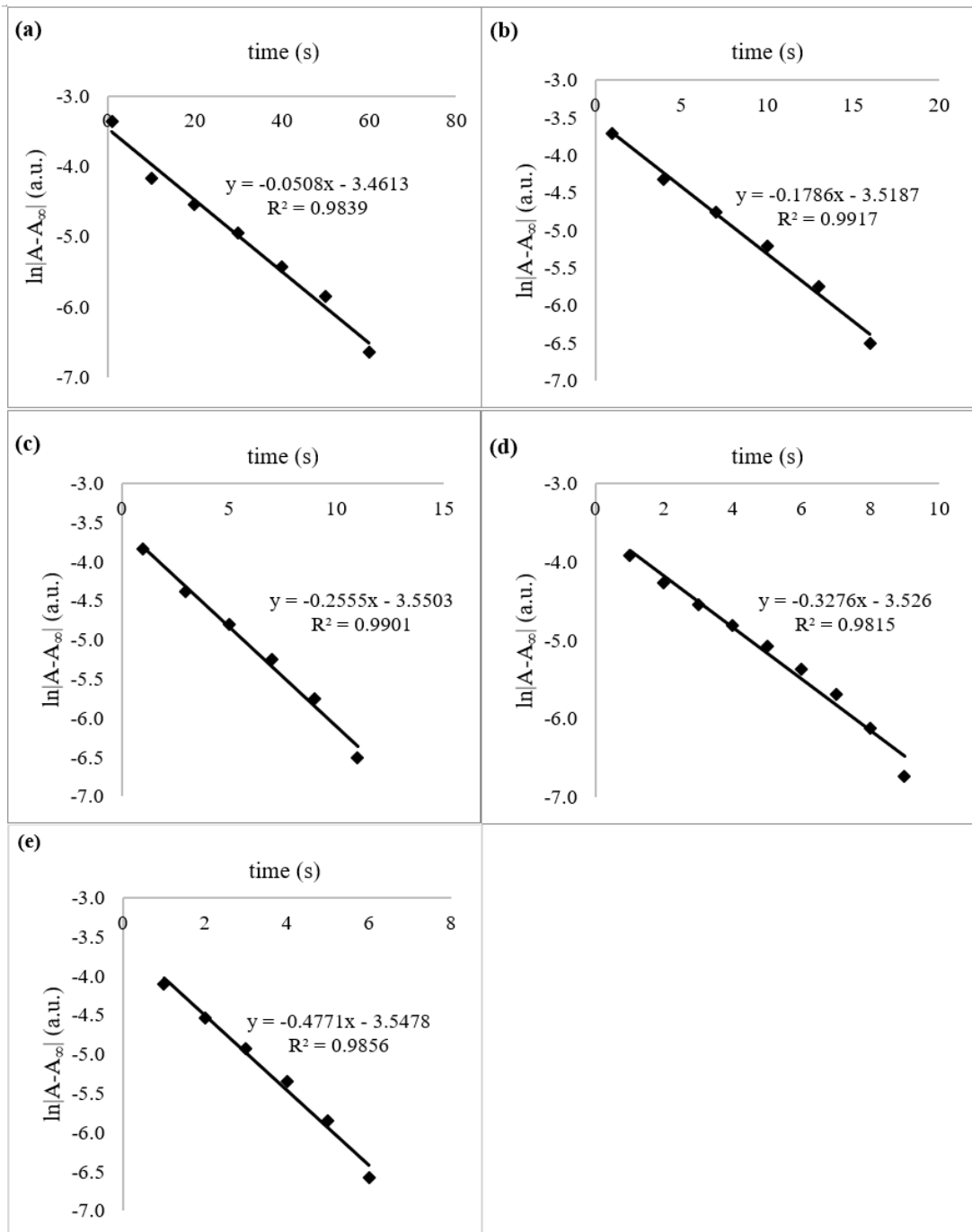


**Figure S7.** Graphs showing  $\ln|A - A_\infty|$  at 420 nm vs time for various concentrations of ethylbenzene used (a to e: 0.024, 0.080, 0.120, 0.160, 0.240 M).

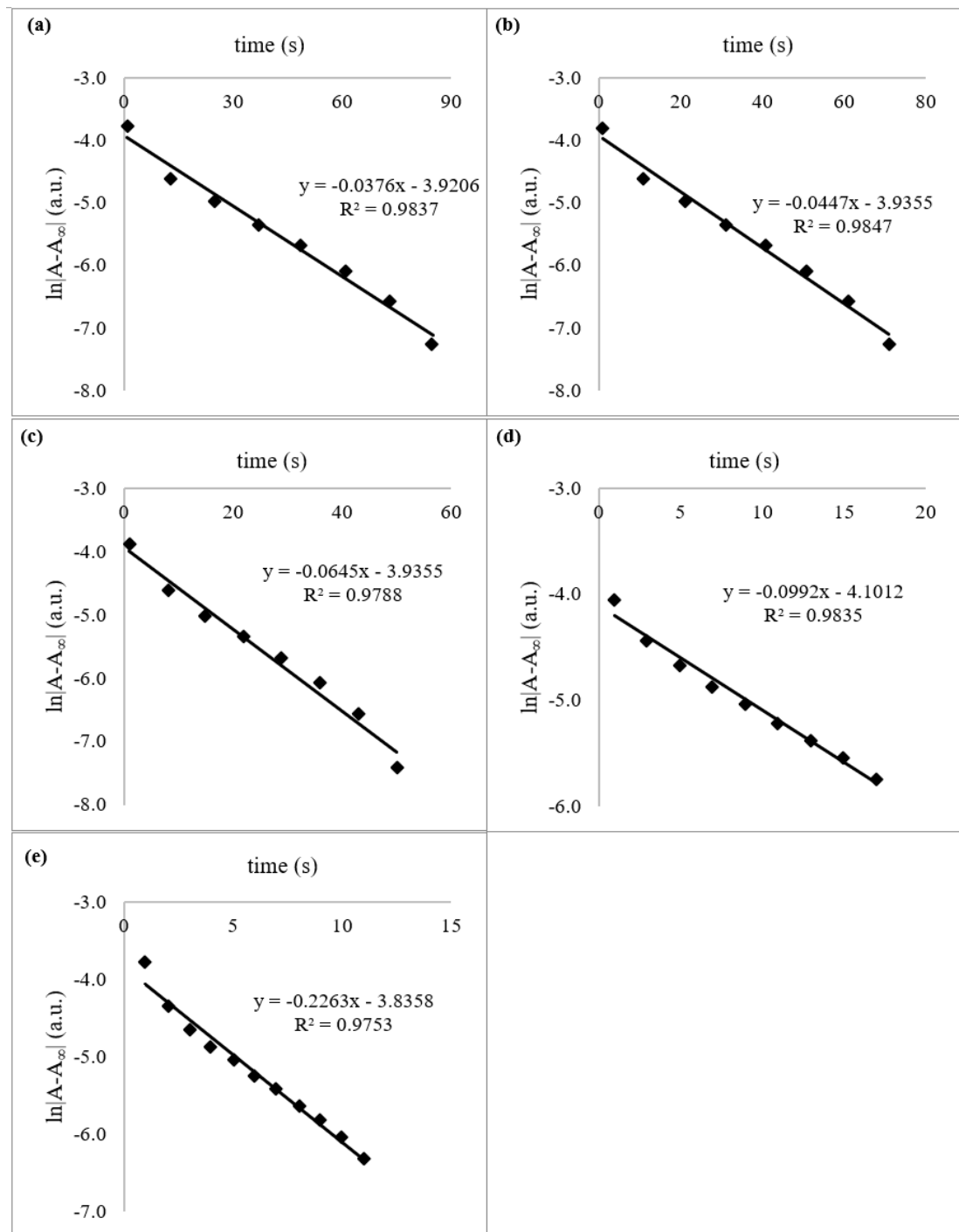


**Figure S8.** Graphs showing  $\ln|A - A_\infty|$  at 420 nm vs time for various concentrations of xanthene used (a to e:  $0.98 \times 10^{-3}$ ,  $1.47 \times 10^{-3}$ ,  $1.95 \times 10^{-3}$ ,  $2.92 \times 10^{-3}$ ,  $6.72 \times 10^{-3}$  M).

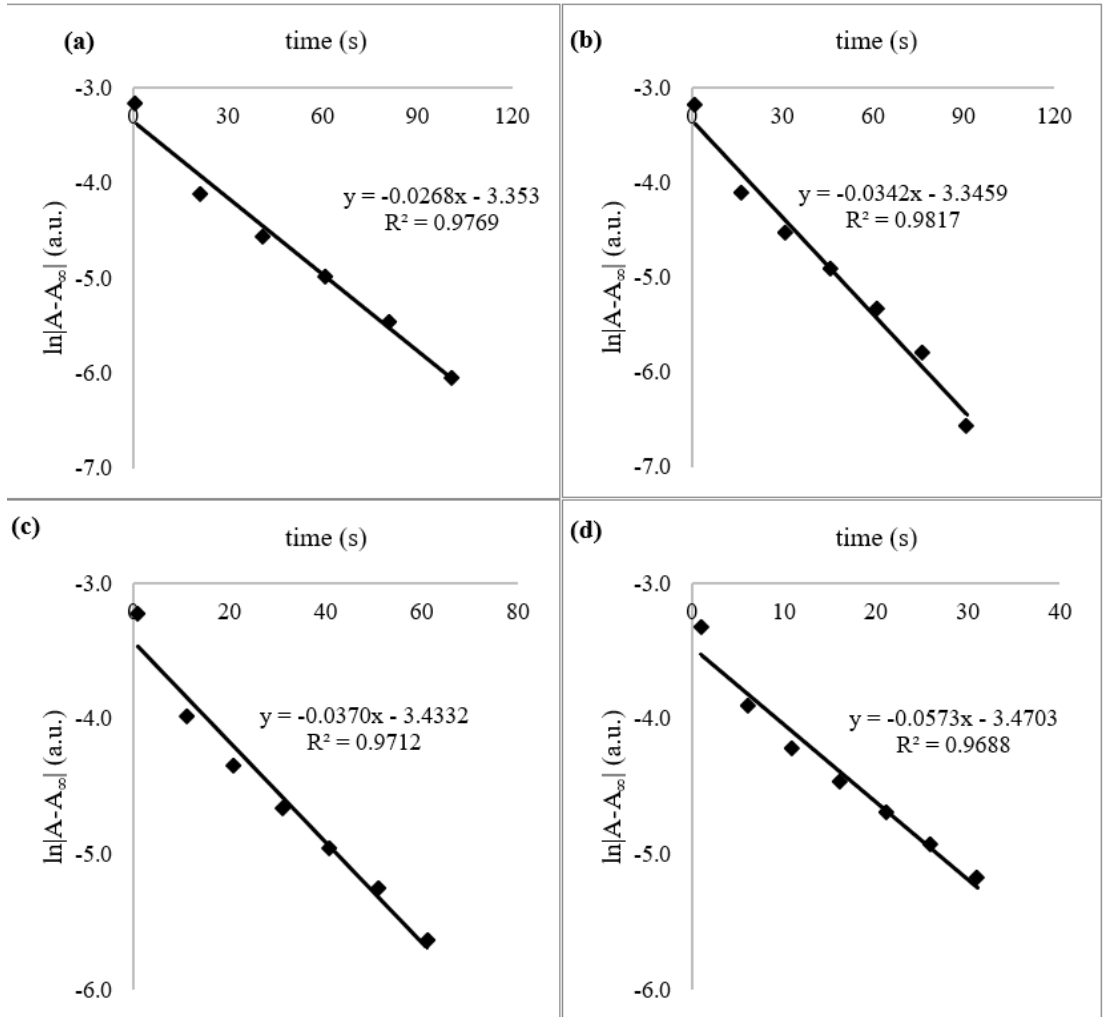


**Figure S9.** Graphs showing  $\ln|A - A_\infty|$  at 420 nm vs time for various concentrations of 9,10-dihydroanthracene used (a to d:  $0.80 \times 10^{-3}$ ,  $1.05 \times 10^{-3}$ ,  $1.13 \times 10^{-3}$ ,  $1.75 \times 10^{-3}$  M).

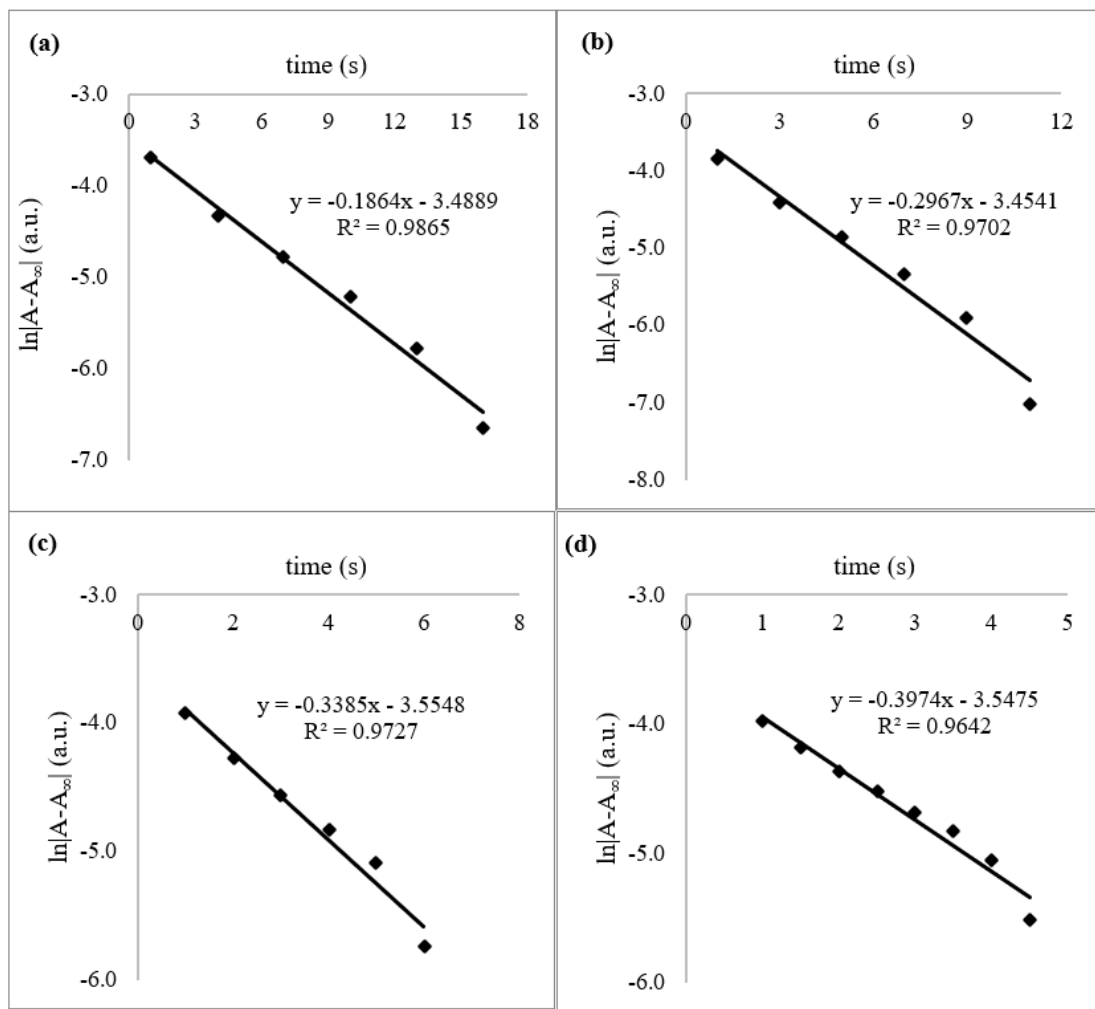


**Figure S10.** Graphs showing  $\ln|A - A_\infty|$  at 420 nm vs time for various concentrations of fluorene used (a to d: 0.020, 0.032, 0.036, 0.042 M).

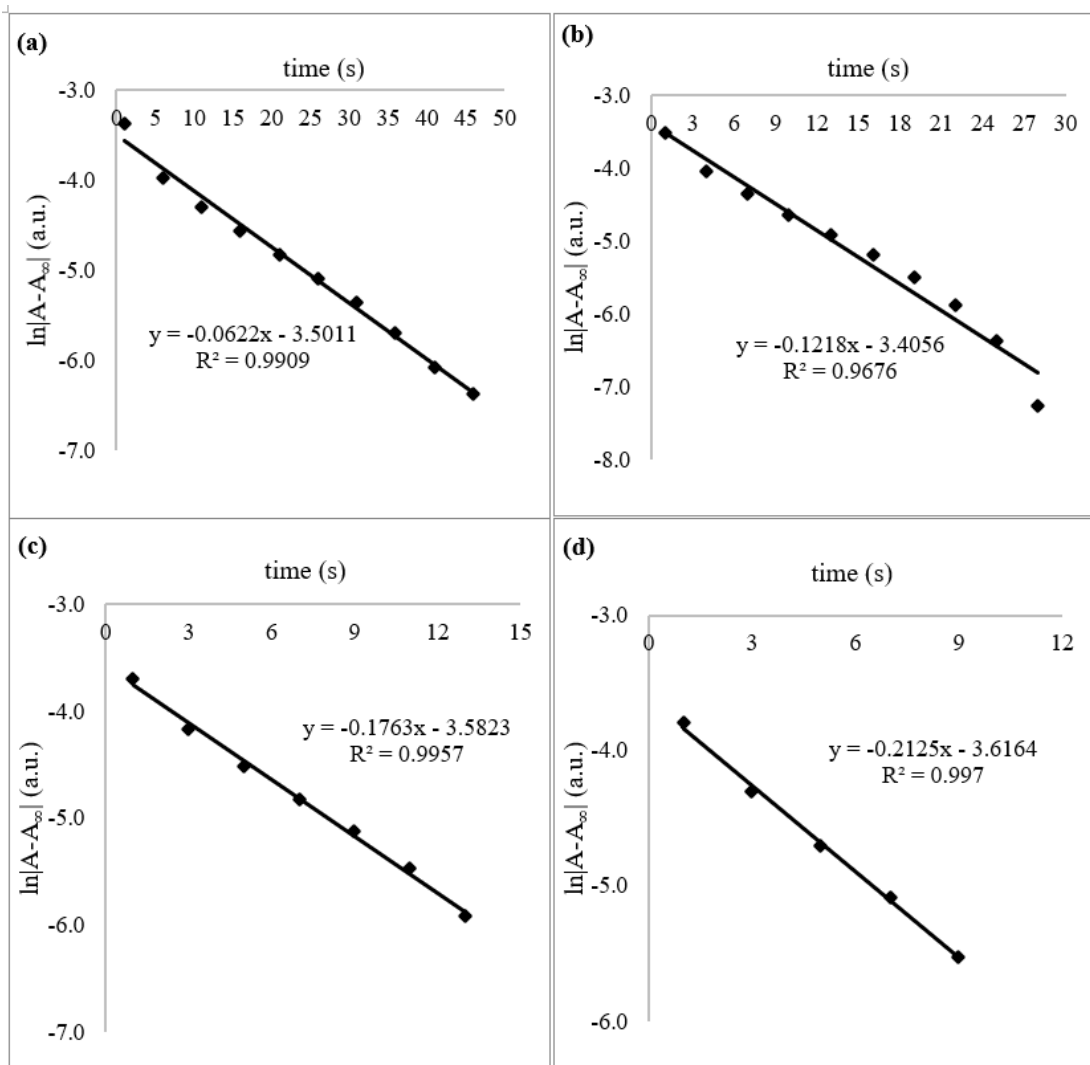


**Figure S11.** Graphs showing  $\ln|A - A_\infty|$  at 420 nm vs time for various concentrations of methylcyclohexane used (a to d: 0.26, 0.52, 0.78, 1.04 M).

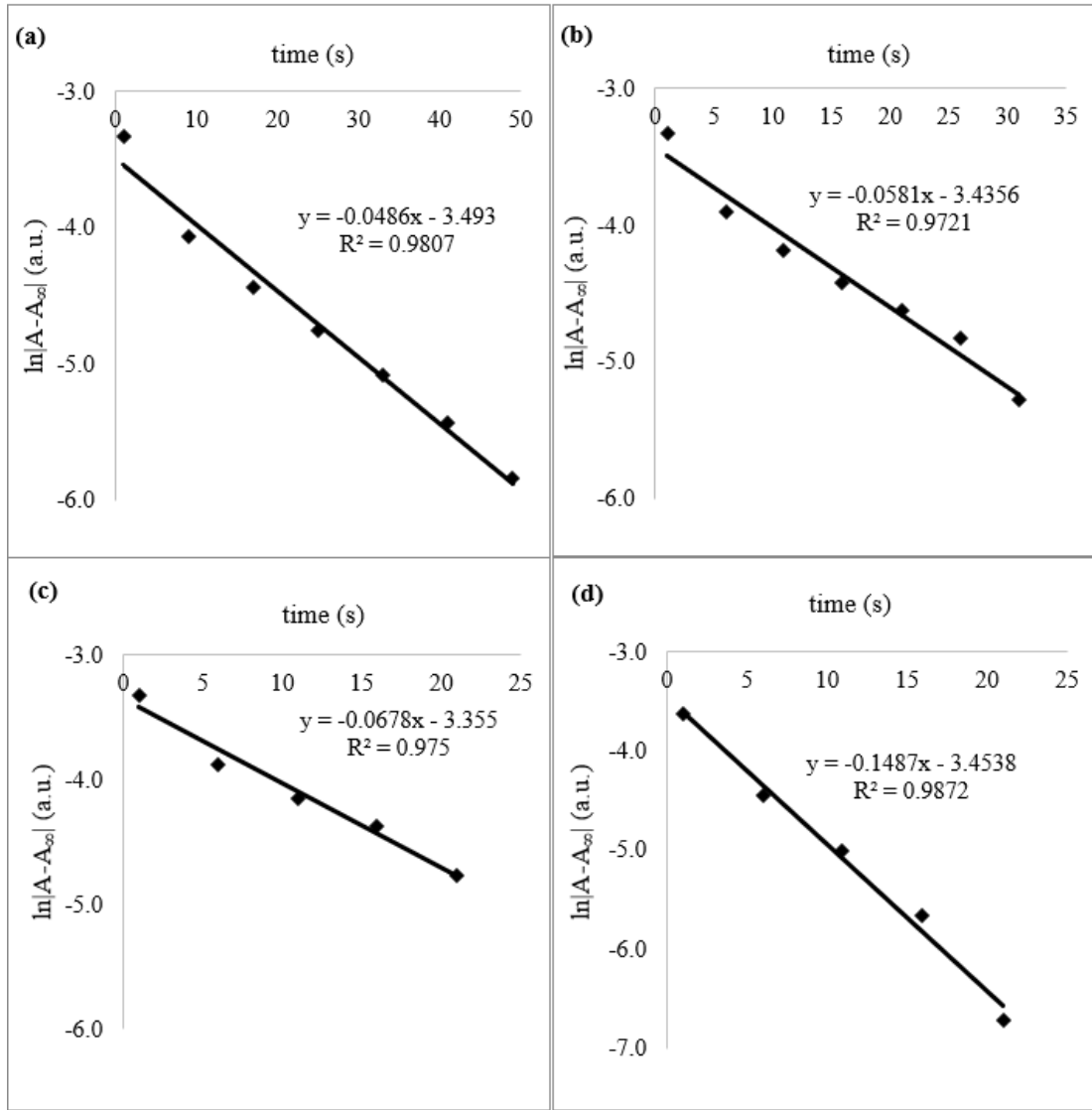


**Figure S12.** Graphs showing  $\ln|A - A_\infty|$  at 420 nm vs time for various concentrations of methylcyclohexane- $d_{14}$  used (a to d: 0.60, 1.19, 1.49, 2.98 M).

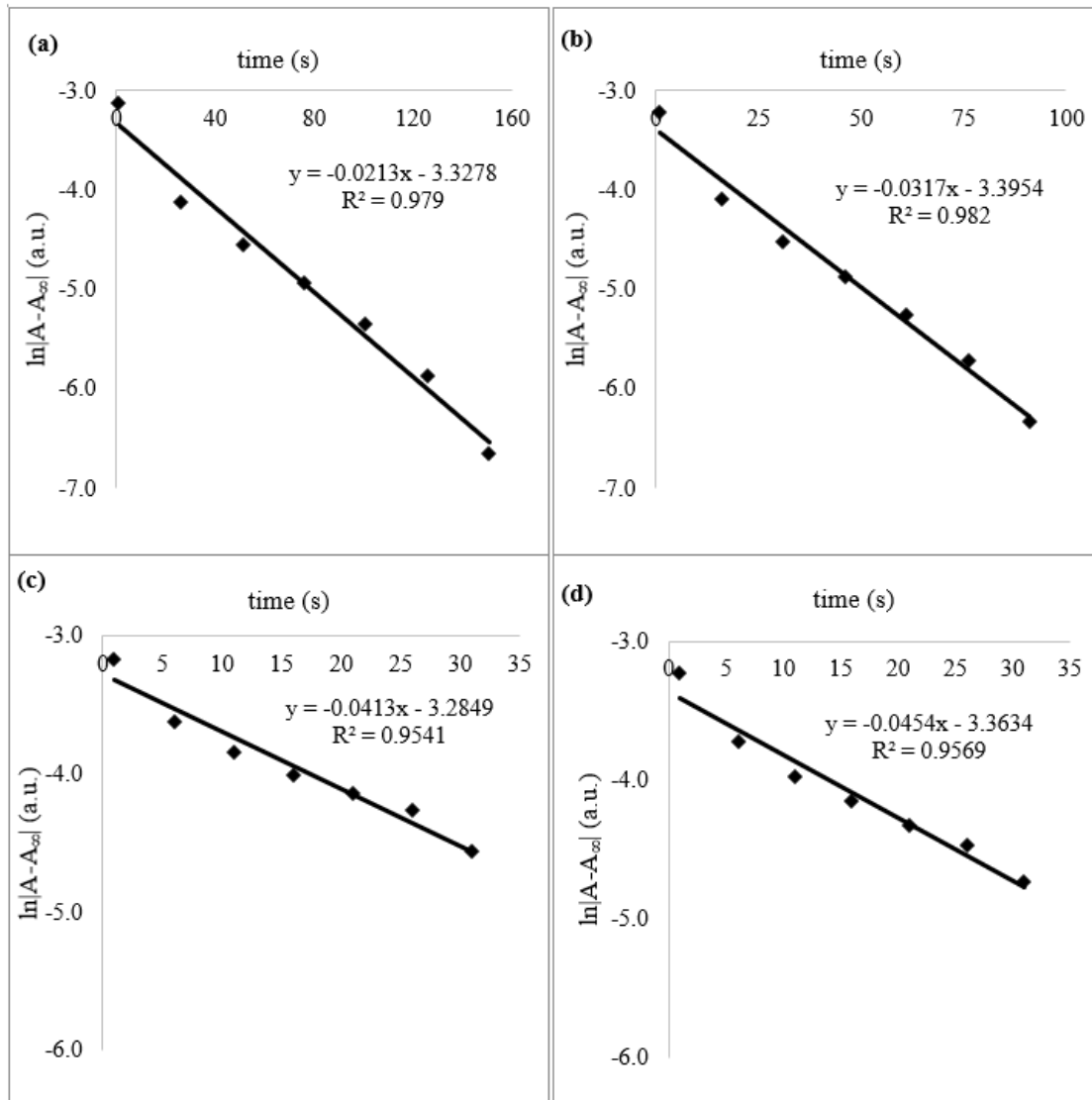


**Figure S13.** Graphs showing  $\ln|A - A_\infty|$  at 420 nm vs time for various concentrations of 1-phenylethanol used (a to d: 0.008, 0.012, 0.016, 0.020 M).

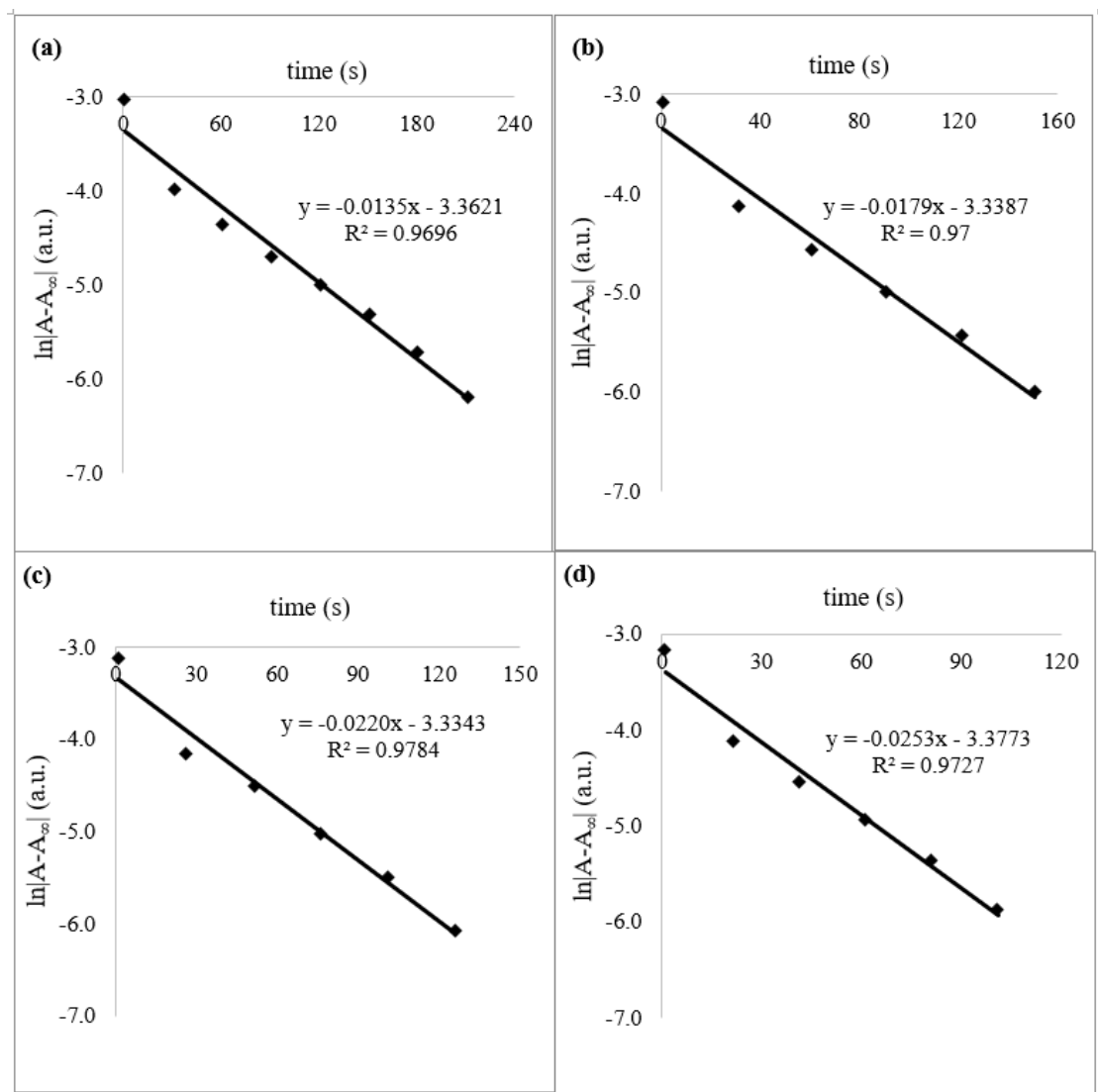


**Figure S14.** Graphs showing  $\ln|A - A_\infty|$  at 420 nm vs time for various concentrations of 1-phenylethanol- $d_{10}$  used (a to d: 0.020, 0.024, 0.027, 0.031 M).

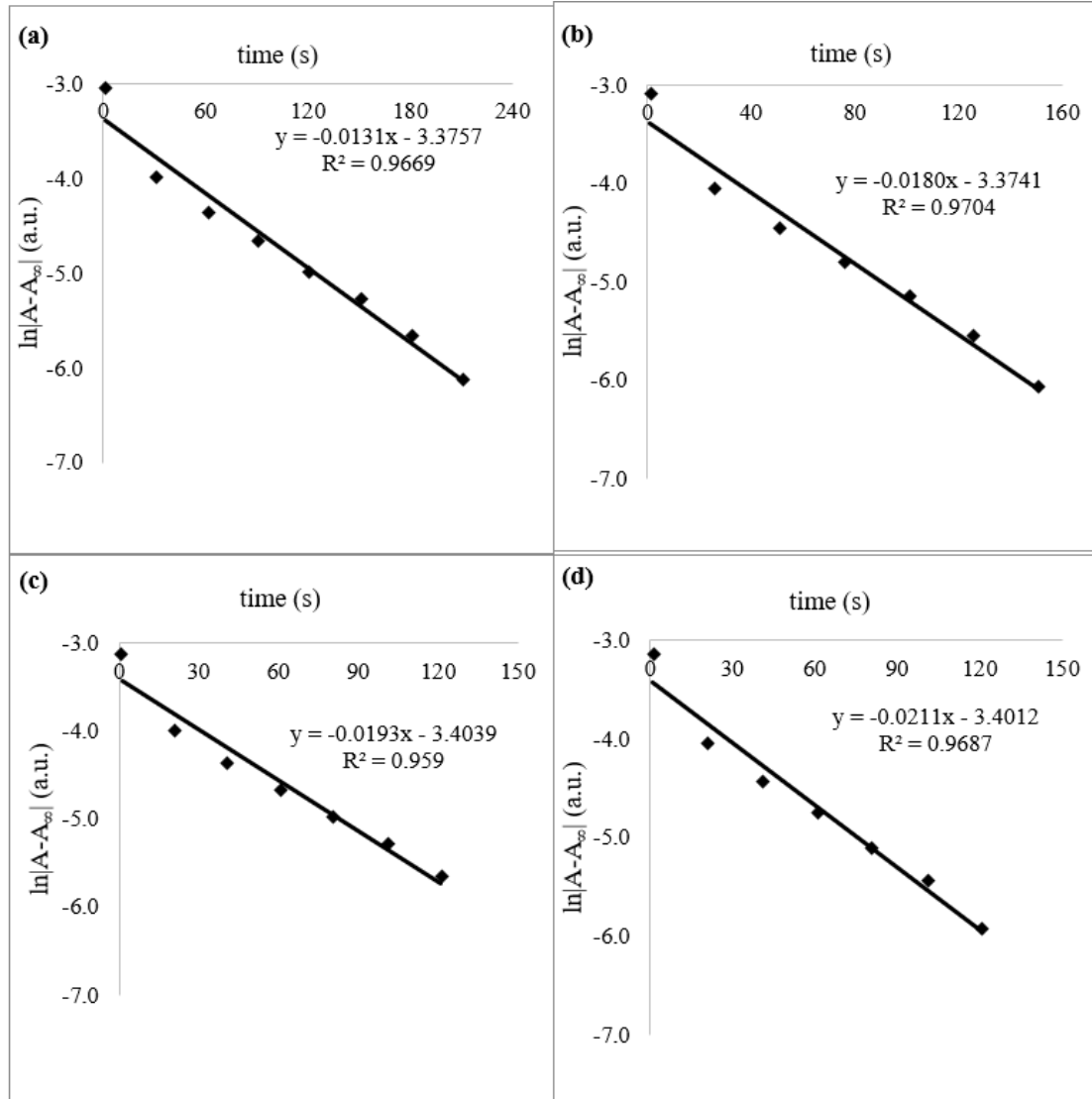


**Figure S15.** Graphs showing  $\ln|A - A_\infty|$  at 420 nm vs time for various concentrations of 1-decene used (a to d:  $0.77 \times 10^{-3}$ ,  $1.02 \times 10^{-3}$ ,  $1.27 \times 10^{-3}$ ,  $1.51 \times 10^{-3}$  M).

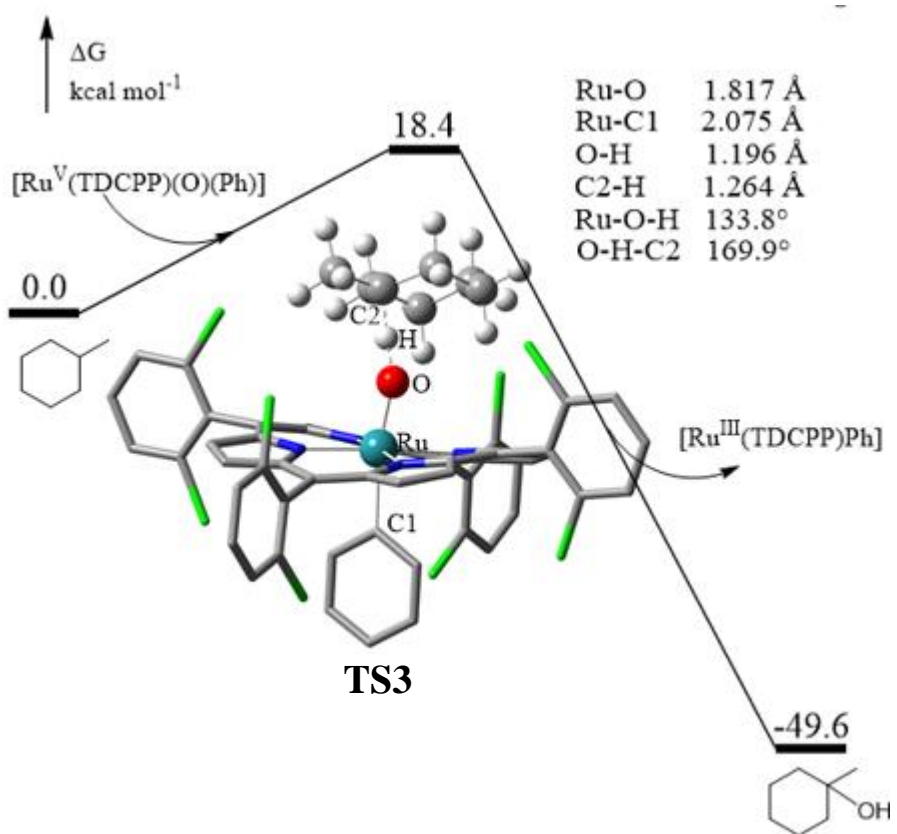


**Figure S16.** Free energy surface of hydroxylation of methylcyclohexane by  $[\text{Ru}^{\text{V}}(\text{TDCPP})(\text{O})(\text{Ph})]$  (<sup>2</sup>A).

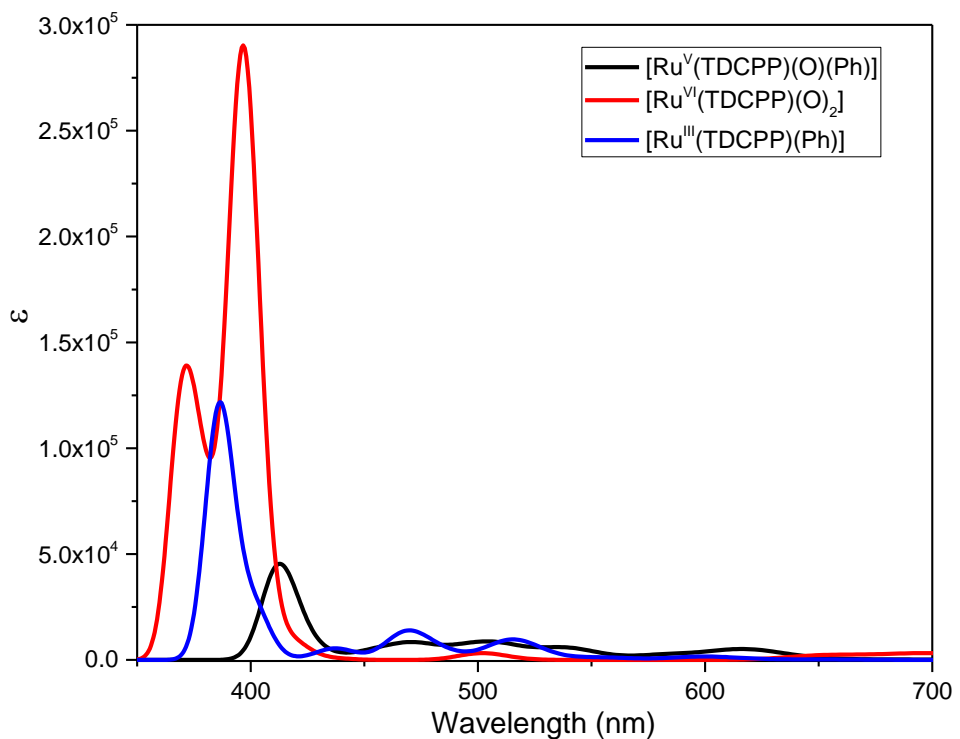


**Figure S17.** TD-DFT simulated UV-vis spectra of  $[\text{Ru}^{\text{V}}(\text{TDCPP})(\text{O})(\text{Ph})]$  ( ${}^2\text{A}$ ),  $[\text{Ru}^{\text{VI}}(\text{TDCPP})(\text{O})_2]$ , and  $[\text{Ru}^{\text{III}}(\text{TDCPP})(\text{Ph})]$ .

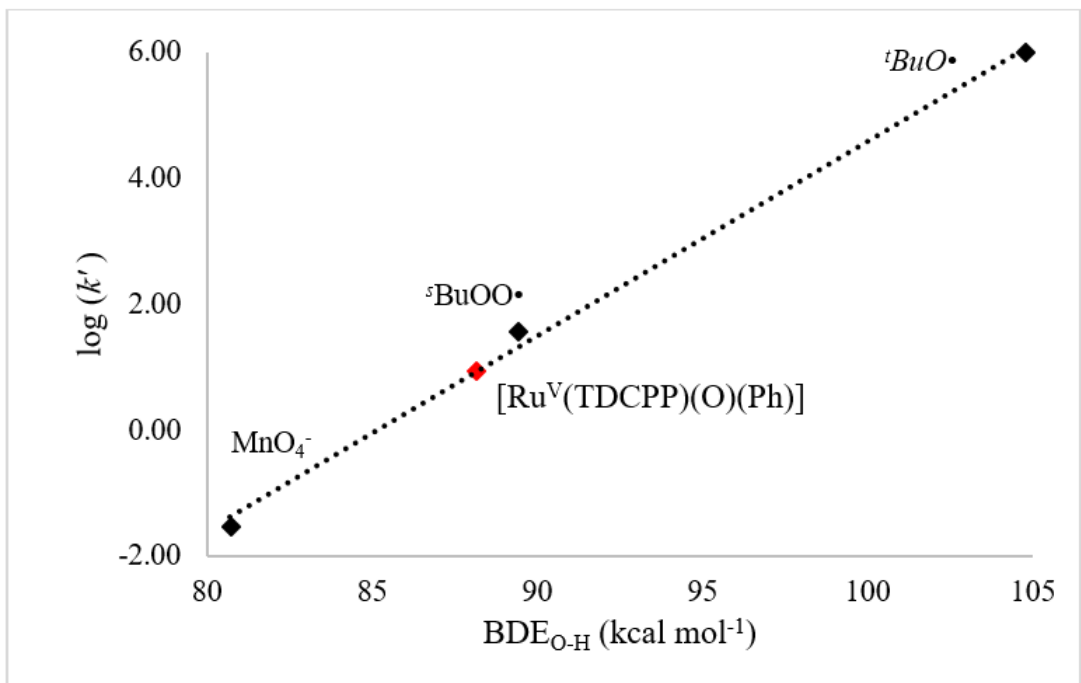


**Figure S18.** Graph showing the Brønsted-Evans-Polanyi relationship.

$k_2$  for  $MnO_4^-$ : Gardner, K. A.; Kuehnert, L. L.; Mayer, J. M. *Inorg. Chem.* **1997**, *36*, 2069.

$k_2$  for  $s\text{BuOO}^\bullet$ : Howard, J. A.; Ingold, K. U. *Can. J. Chem.* **1968**, *46*, 2661. The  $k_2$  at 303 K was used, assuming the effect of small temperature change on the  $k_2$  is negligible (see: Wang, K.; Mayer, J. M. *J. Am. Chem. Soc.* **1997**, *119*, 1470).

$k_2$  for  $t\text{BuO}^\bullet$ : Mulder, P.; Arends, I. W. C. E.; Clark, K. B.; Wayner, D. D. M. *J. Phys. Chem.* **1995**, *99*, 8182.

BDE of  $[MnO_3O-H]^-$ : Gardner, K. A.; Kuehnert, L. L.; Mayer, J. M. *Inorg. Chem.* **1997**, *36*, 2069.

BDE of  $s\text{BuOO-H}$  and  $t\text{BuO-H}$ : Colussi, A. J. *In Chemical Kinetics of Small Organic Radicals*; Alfassi, Z. B., Ed.; CRC Press: Boca Raton, FL, 1988; p 33 (the BDE of  $s\text{BuOO-H}$  is taken as the same value as that of  $s\text{BuOOH}$ ).

## Cartesian Coordinates

[Ru<sup>V</sup>(TDCPP)(O)(Ph)] (<sup>2</sup>A, S = 1/2)

Center Number	Atomic Number	Atomic Type	Coordinates (Angstroms)		
			X	Y	Z
1	44	0	-0.03063	0.06646	-0.35251
2	17	0	-4.99466	0.11408	2.10472
3	17	0	0.03529	4.48717	2.87546
4	17	0	4.41377	-0.04265	-3.26455
5	17	0	5.10182	0.09328	2.05822
6	17	0	0.00571	5.10972	-2.4547
7	7	0	-1.4731	-1.37322	-0.40104
8	7	0	1.43726	-1.41463	-0.30539
9	7	0	-1.42813	1.47076	-0.22519
10	7	0	1.43148	1.47464	-0.18634
11	17	0	-4.58747	0.05579	-3.24574
12	17	0	-0.00853	-4.12238	2.69569
13	17	0	-0.08906	-5.23179	-2.54248
14	6	0	1.2532	2.80068	-0.0322
15	6	0	2.76427	1.26069	-0.30388
16	6	0	-1.26822	-2.70584	-0.27508
17	6	0	0.14034	-0.4052	1.69614
18	6	0	2.52047	3.46954	-0.03245
19	1	0	2.66837	4.54762	0.08047
20	6	0	1.2189	-2.73664	-0.24094
21	6	0	4.86471	0.02326	-0.62048
22	6	0	-2.80231	-1.1793	-0.47687
23	6	0	2.75972	-1.2217	-0.43005
24	6	0	-0.0356	-3.34611	-0.16675
25	6	0	0.01546	3.4372	0.0555
26	6	0	-1.06809	-0.52038	2.38658
27	1	0	-2.03663	-0.46752	1.86724
28	6	0	-1.21969	2.80893	-0.05293
29	6	0	0.01966	4.9087	0.22369
30	6	0	2.47252	-3.43536	-0.29404
31	1	0	2.59586	-4.5219	-0.25662
32	6	0	3.39242	0.02527	-0.45192
33	6	0	-2.52999	-3.38732	-0.284
34	1	0	-2.66411	-4.47016	-0.20324
35	6	0	-3.48579	-2.4381	-0.42874
36	1	0	-4.5701	-2.57422	-0.48087
37	6	0	-3.43581	2.54867	-0.23267
38	1	0	-4.51758	2.7003	-0.29356
39	6	0	-4.90399	0.08877	-0.57987
40	6	0	-2.77718	1.2889	-0.33232
41	6	0	-0.03884	-5.26574	1.42078
42	6	0	-0.05233	-6.62002	1.72017
43	1	0	-0.04123	-6.9392	2.76919
44	6	0	3.46014	2.51188	-0.21749
45	1	0	4.54476	2.63844	-0.28486
46	6	0	-5.7223	0.10797	0.55129
47	6	0	5.74106	0.04287	0.46618
48	6	0	-2.47232	3.48801	-0.04756
49	1	0	-2.60215	4.56765	0.07276
50	6	0	-7.6985	0.11428	-0.79058

51	1	0	-8.79388	0.12518	-0.87187
52	6	0	-0.07851	-5.76159	-0.91181
53	6	0	7.11833	0.02123	0.30533
54	1	0	7.76491	0.03681	1.191
55	6	0	0.02003	5.77206	-0.8747
56	6	0	6.8166	-0.0417	-2.0799
57	1	0	7.22062	-0.07344	-3.09913
58	6	0	0.03463	5.49977	1.49017
59	6	0	0.03479	7.15112	-0.72686
60	1	0	0.03569	7.78805	-1.61954
61	6	0	1.32739	-0.4935	2.41848
62	1	0	2.3016	-0.41799	1.91643
63	6	0	-6.92666	0.09315	-1.93868
64	1	0	-7.38317	0.08744	-2.93591
65	6	0	1.31128	-0.66602	3.79495
66	1	0	2.26271	-0.72726	4.34426
67	6	0	-3.42746	0.06917	-0.47923
68	6	0	-5.54451	0.08006	-1.8222
69	6	0	-0.05329	-4.80282	0.10211
70	6	0	3.43344	-2.49005	-0.43401
71	1	0	4.51434	-2.636	-0.52211
72	6	0	5.44191	-0.0184	-1.89373
73	6	0	0.10617	-0.76601	4.4752
74	1	0	0.09364	-0.90998	5.56513
75	6	0	-7.10599	0.1217	0.46073
76	1	0	-7.70636	0.13697	1.3782
77	6	0	7.6465	-0.02236	-0.9732
78	1	0	8.73631	-0.04123	-1.1098
79	6	0	0.05006	7.69343	0.54652
80	1	0	0.06286	8.78474	0.67149
81	6	0	0.04978	6.87616	1.66291
82	1	0	0.06131	7.29172	2.6779
83	6	0	-1.08123	-0.68259	3.76746
84	1	0	-2.04586	-0.75708	4.29177
85	6	0	-0.08007	-7.53854	0.68484
86	1	0	-0.09132	-8.61315	0.91336
87	6	0	-0.09263	-7.12158	-0.63499
88	1	0	-0.11229	-7.84174	-1.46224
89	8	0	0.33696	-0.17941	-2.01614

**[Ru<sup>VI</sup>(TDCPP)O<sub>2</sub>] (S = 0)**

Center Number	Atomic Number	Atomic Type	Coordinates (Angstroms)		
			X	Y	Z
1	44	0	0.02310	0.00020	0.00002
2	17	0	0.00443	4.78272	2.68112
3	17	0	4.79039	-0.00173	2.68148
4	17	0	0.00213	-4.78247	-2.68115
5	17	0	0.00158	-4.78261	2.68102
6	17	0	4.79034	-0.00110	-2.68131
7	7	0	-1.44941	1.45731	0.00001
8	7	0	-1.45042	-1.45643	-0.00002
9	7	0	1.45103	1.44116	0.00006
10	7	0	1.45031	-1.44203	0.00002
11	17	0	0.00503	4.78258	-2.68107

12	17	0	-4.77840	0.00133	2.68070
13	17	0	-4.77848	0.00161	-2.68079
14	6	0	2.78694	-1.23895	0.00005
15	6	0	1.23577	-2.77896	-0.00001
16	6	0	-2.77938	1.24306	-0.00002
17	6	0	3.45775	-2.50111	0.00003
18	1	0	4.54303	-2.64022	0.00004
19	6	0	-2.78020	-1.24147	-0.00004
20	6	0	0.00201	-4.90031	-0.00007
21	6	0	-1.24400	2.78641	0.00002
22	6	0	-1.24570	-2.78561	-0.00003
23	6	0	-3.41376	0.00101	-0.00004
24	6	0	3.42574	-0.00103	0.00008
25	6	0	2.78763	1.23720	0.00008
26	6	0	4.90766	-0.00143	0.00008
27	6	0	-3.46407	-2.50256	-0.00005
28	1	0	-4.55039	-2.63407	-0.00006
29	6	0	-0.00206	-3.41788	-0.00004
30	6	0	-3.46249	2.50453	-0.00002
31	1	0	-4.54873	2.63664	-0.00003
32	6	0	-2.50708	3.46529	0.00001
33	1	0	-2.64398	4.55091	0.00001
34	6	0	2.49695	3.45530	0.00008
35	1	0	2.62993	4.54136	0.00007
36	6	0	0.00492	4.90041	0.00002
37	6	0	1.23740	2.77830	0.00006
38	6	0	-5.62672	0.00165	1.19048
39	6	0	-7.01374	0.00209	1.20305
40	1	0	-7.54309	0.00221	2.16358
41	6	0	2.49490	-3.45683	0.00001
42	1	0	2.62717	-4.54299	-0.00001
43	6	0	0.00544	5.63068	1.19050
44	6	0	0.00212	-5.63058	1.19041
45	6	0	3.45917	2.49893	0.00010
46	1	0	4.54455	2.63735	0.00011
47	6	0	0.00797	7.70169	-0.00005
48	1	0	0.00908	8.80042	-0.00007
49	6	0	-5.62675	0.00176	-1.19054
50	6	0	0.00289	-7.01757	1.20297
51	1	0	0.00284	-7.54705	2.16342
52	6	0	5.63808	-0.00152	-1.19042
53	6	0	0.00313	-7.01750	-1.20323
54	1	0	0.00328	-7.54693	-2.16371
55	6	0	5.63809	-0.00176	1.19056
56	6	0	7.02505	-0.00193	-1.20307
57	1	0	7.55459	-0.00199	-2.16348
58	6	0	0.00734	7.01761	-1.20313
59	1	0	0.00784	7.54705	-2.16361
60	6	0	-0.00001	3.41799	0.00004
61	6	0	0.00568	5.63063	-1.19050
62	6	0	-4.89661	0.00149	-0.00003
63	6	0	-2.50919	-3.46383	-0.00006
64	1	0	-2.64669	-4.54938	-0.00008
65	6	0	0.00234	-5.63052	-1.19059
66	6	0	0.00707	7.01767	1.20307
67	1	0	0.00736	7.54715	2.16352
68	6	0	0.00333	-7.70159	-0.00015
69	1	0	0.00376	-8.80032	-0.00018
70	6	0	7.70905	-0.00228	0.00006
71	1	0	8.80778	-0.00262	0.00005

72	6	0	7.02506	-0.00219	1.20320
73	1	0	7.55462	-0.00248	2.16360
74	6	0	-7.69786	0.00237	0.00000
75	1	0	-8.79660	0.00273	0.00001
76	6	0	-7.01377	0.00221	-1.20307
77	1	0	-7.54314	0.00244	-2.16359
78	8	0	-0.14097	-0.00123	-1.68337
79	8	0	-0.14102	-0.00127	1.68341

---

**[Ru<sup>III</sup>(TDCPP)(Ph)] (S = 1/2)**

Center Number	Atomic Number	Atomic Type	Coordinates (Angstroms)		
			X	Y	Z
1	44	0	-0.00503	0.02431	-0.23059
2	17	0	5.07764	0.07106	1.97677
3	17	0	-0.12778	-4.03626	2.68873
4	17	0	-4.5218	0.04473	-3.29413
5	17	0	-5.03737	0.37425	2.04216
6	17	0	-0.21198	-5.32689	-2.51553
7	7	0	1.48539	1.40591	-0.25596
8	7	0	-1.37381	1.49614	-0.28127
9	7	0	1.36319	-1.43587	-0.45022
10	7	0	-1.4939	-1.34706	-0.3946
11	17	0	4.45956	-0.34002	-3.34551
12	17	0	0.39313	4.42699	2.79654
13	17	0	-0.02661	5.12219	-2.50777
14	6	0	-1.34978	-2.6897	-0.29277
15	6	0	-2.82477	-1.11083	-0.48633
16	6	0	1.34159	2.74669	-0.12226
17	6	0	0.00143	-0.204	1.7339
18	6	0	-2.63389	-3.33167	-0.32583
19	1	0	-2.80555	-4.41123	-0.27134
20	6	0	-1.13092	2.82622	-0.12345
21	6	0	-4.886	0.21098	-0.63784
22	6	0	2.81466	1.17748	-0.40475
23	6	0	-2.72585	1.35766	-0.38409
24	6	0	0.1287	3.4163	-0.02079
25	6	0	-0.13506	-3.35736	-0.20202
26	6	0	1.213	-0.28442	2.42645
27	1	0	2.16961	-0.15603	1.89889
28	6	0	1.12261	-2.76868	-0.32742
29	6	0	-0.1733	-4.80274	0.1152
30	6	0	-2.35917	3.54694	-0.12326
31	1	0	-2.45933	4.63061	-0.00764
32	6	0	-3.41141	0.14937	-0.5073
33	6	0	2.62392	3.39215	-0.17264
34	1	0	2.79537	4.47023	-0.09426
35	6	0	3.53998	2.4166	-0.36186
36	1	0	4.62399	2.52168	-0.46853
37	6	0	3.34299	-2.56755	-0.49069
38	1	0	4.42106	-2.74727	-0.5473
39	6	0	4.87242	-0.13222	-0.69827
40	6	0	2.7137	-1.29037	-0.52671
41	6	0	0.29431	5.45754	1.42953
42	6	0	0.33915	6.83106	1.61884

43	1	0	0.43177	7.23115	2.63592
44	6	0	-3.55209	-2.34923	-0.46936
45	1	0	-4.63909	-2.44888	-0.54787
46	6	0	5.73725	-0.0714	0.39678
47	6	0	-5.72882	0.30818	0.4713
48	6	0	2.35121	-3.48808	-0.3447
49	1	0	2.45248	-4.57483	-0.2639
50	6	0	7.65879	-0.24216	-1.01165
51	1	0	8.74982	-0.28463	-1.13389
52	6	0	0.10895	5.76637	-0.92188
53	6	0	-7.10943	0.35906	0.34994
54	1	0	-7.72706	0.43517	1.2531
55	6	0	-0.20847	-5.79571	-0.86317
56	6	0	-6.88067	0.2135	-2.03949
57	1	0	-7.31535	0.1748	-3.04575
58	6	0	-0.17008	-5.22247	1.44916
59	6	0	-0.24049	-7.14502	-0.5431
60	1	0	-0.26866	-7.89016	-1.34749
61	6	0	-1.19434	-0.36421	2.44035
62	1	0	-2.16487	-0.29019	1.92822
63	6	0	6.84116	-0.30885	-2.12587
64	1	0	7.25642	-0.40233	-3.13671
65	6	0	-1.17264	-0.60808	3.80487
66	1	0	-2.12208	-0.72743	4.34781
67	6	0	3.39973	-0.07498	-0.5472
68	6	0	5.46565	-0.25414	-1.95757
69	6	0	0.17593	4.88627	0.16035
70	6	0	-3.35199	2.63388	-0.30062
71	1	0	-4.42897	2.81887	-0.35974
72	6	0	-5.50268	0.16524	-1.8907
73	6	0	0.03445	-0.71888	4.48036
74	1	0	0.04777	-0.92902	5.55949
75	6	0	7.11586	-0.12417	0.25574
76	1	0	7.75078	-0.07371	1.1486
77	6	0	-7.67627	0.31065	-0.91153
78	1	0	-8.76905	0.34996	-1.01817
79	6	0	-0.23606	-7.51851	0.78977
80	1	0	-0.26073	-8.58473	1.05423
81	6	0	-0.20096	-6.56573	1.79348
82	1	0	-0.19716	-6.8504	2.85273
83	6	0	1.22474	-0.5545	3.78594
84	1	0	2.18727	-0.63529	4.31279
85	6	0	0.26593	7.66566	0.51758
86	1	0	0.30082	8.75488	0.65774
87	6	0	0.15175	7.14293	-0.75888
88	1	0	0.09681	7.79187	-1.64134

### Ethylbenzene

Center Number	Atomic Number	Atomic Type	X	Y	Z
1	6	0	-0.6815	-6.21441	9.78804
2	6	0	-1.92452	-6.31426	8.95291

3	1	0	0.16463	-6.73355	9.30582
4	1	0	-0.36503	-5.16662	9.94569
5	1	0	-0.81115	-6.67124	10.78701
6	1	0	-1.72832	-5.89368	7.94342
7	1	0	-2.15423	-7.38276	8.75471
8	6	0	-3.15942	-5.66664	9.50054
9	6	0	-3.17257	-4.94923	10.69339
10	6	0	-4.35915	-5.77684	8.79451
11	6	0	-4.34092	-4.36391	11.16361
12	1	0	-2.2498	-4.839	11.28058
13	6	0	-5.52489	-5.19612	9.25987
14	1	0	-4.37374	-6.33952	7.8477
15	6	0	-5.52171	-4.48348	10.45117
16	1	0	-4.32315	-3.80313	12.10913
17	1	0	-6.45467	-5.30104	8.68274
18	1	0	-6.44545	-4.01954	10.82394

### 1-Phenylethanol

Center Number	Atomic Number	Atomic Type	Coordinates (Angstroms)		
			X	Y	Z
1	8	0	-2.74665	-0.00216	9.67014
2	6	0	-2.7892	-2.1917	10.43425
3	6	0	-3.59721	-1.08179	9.81833
4	1	0	-1.91208	-2.42307	9.80514
5	1	0	-2.42283	-1.89122	11.43283
6	1	0	-3.38821	-3.10989	10.5525
7	1	0	-3.24889	0.71849	9.28782
8	1	0	-3.96686	-1.43733	8.82113
9	6	0	-4.81091	-0.7491	10.65054
10	6	0	-4.73907	0.23306	11.63398
11	6	0	-6.00888	-1.43533	10.47452
12	6	0	-5.8422	0.52087	12.42346
13	1	0	-3.79424	0.77886	11.77327
14	6	0	-7.11052	-1.15298	11.26567
15	1	0	-6.07864	-2.20642	9.69045
16	6	0	-7.0298	-0.17185	12.24358
17	1	0	-5.77442	1.30006	13.19624
18	1	0	-8.05028	-1.70231	11.11208
19	1	0	-7.90409	0.05586	12.86941

### Methylcyclohexane

Center Number	Atomic Number	Atomic Type	Coordinates (Angstroms)		
			X	Y	Z
1	6	0	-1.52553	-2.64348	12.51536
2	1	0	-1.96207	-1.68763	12.8593
3	1	0	-0.43625	-2.48727	12.40829
4	1	0	-1.66903	-3.37843	13.33238
5	6	0	-2.15547	-3.12263	11.23471
6	6	0	-1.52577	-4.41033	10.73753
7	6	0	-3.65684	-3.29226	11.36863
8	1	0	-1.98062	-2.34647	10.45005
9	6	0	-2.16115	-4.90884	9.46171

10	1	0	-1.6296	-5.18563	11.53173
11	1	0	-0.43317	-4.27312	10.60377
12	6	0	-4.29788	-3.78817	10.09477
13	1	0	-4.12	-2.33867	11.69543
14	1	0	-3.85938	-4.01566	12.1922
15	6	0	-3.65567	-5.06708	9.61109
16	1	0	-1.69575	-5.8616	9.14106
17	1	0	-1.94985	-4.18722	8.64173
18	1	0	-5.3884	-3.92494	10.23475
19	1	0	-4.19797	-3.00832	9.30744
20	1	0	-3.8663	-5.88093	10.3405
21	1	0	-4.11233	-5.39916	8.65793

---

## TS1 ( $S = 1/2$ )

Center Number	Atomic Number	Atomic Type	Coordinates (Angstroms)		
			X	Y	Z
1	44	0	0.24283	0.02257	-0.05212
2	17	0	4.27205	-3.31098	-1.78327
3	17	0	3.13354	3.37001	-2.65374
4	17	0	-3.57721	2.62925	2.49451
5	17	0	-3.39716	3.36219	-2.82295
6	17	0	3.33311	4.06839	2.66002
7	7	0	0.47111	-1.96103	-0.14325
8	7	0	-1.71675	-0.1763	-0.54873
9	7	0	2.21489	0.24522	0.35302
10	7	0	0.01831	2.06993	-0.022
11	17	0	3.47429	-2.58448	3.48534
12	17	0	-1.84588	-2.82594	-3.94644
13	17	0	-3.19743	-4.39557	1.01299
14	6	0	1.00347	2.97851	0.04702
15	6	0	-1.15049	2.73342	-0.03758
16	6	0	-0.45378	-2.86812	-0.56351
17	6	0	0.71064	0.45374	-2.04083
18	6	0	0.44164	4.30069	0.06539
19	1	0	1.00854	5.2349	0.12138
20	6	0	-2.34533	-1.31091	-0.91618
21	6	0	-3.58152	3.05186	-0.15793
22	6	0	1.58667	-2.66017	0.20225
23	6	0	-2.64784	0.80635	-0.50829
24	6	0	-1.75235	-2.57574	-0.97092
25	6	0	2.36575	2.6799	0.13295
26	6	0	1.83988	-0.15964	-2.59554
27	1	0	2.4904	-0.80969	-1.98849
28	6	0	2.90746	1.41063	0.32064
29	6	0	3.30926	3.81162	-0.01239
30	6	0	-3.73362	-1.04553	-1.14648
31	1	0	-4.47957	-1.7823	-1.45954
32	6	0	-2.40665	2.15109	-0.22143
33	6	0	0.09175	-4.18495	-0.46986
34	1	0	-0.42879	-5.1082	-0.74143
35	6	0	1.34672	-4.05803	0.02972
36	1	0	2.06493	-4.85442	0.24693
37	6	0	4.41472	-0.18746	0.74908
38	1	0	5.32508	-0.75783	0.95869
39	6	0	3.91955	-3.04218	0.87219
40	6	0	3.10146	-0.74075	0.59331
41	6	0	-2.67719	-3.88589	-2.88913
42	6	0	-3.43333	-4.91541	-3.4314
43	1	0	-3.48423	-5.0277	-4.52116
44	6	0	-0.90397	4.14575	0.04025
45	1	0	-1.67071	4.92592	0.05463
46	6	0	4.64881	-3.66495	-0.14549
47	6	0	-4.12044	3.66009	-1.29342
48	6	0	4.29623	1.14887	0.5548
49	1	0	5.08694	1.90423	0.58522
50	6	0	6.00493	-4.83725	1.43411
51	1	0	6.81752	-5.54295	1.65401
52	6	0	-3.26964	-4.5818	-0.69286
53	6	0	-5.22076	4.50164	-1.23063
54	1	0	-5.60588	4.95627	-2.15144
55	6	0	3.8144	4.52284	1.07703

56	6	0	-5.30138	4.17409	1.15105
57	1	0	-5.75283	4.36784	2.13164
58	6	0	3.72413	4.21526	-1.28581
59	6	0	4.69231	5.58566	0.91778
60	1	0	5.0662	6.11325	1.80325
61	6	0	-0.06298	1.26364	-2.87304
62	1	0	-0.96117	1.76947	-2.48671
63	6	0	5.32438	-4.22996	2.47417
64	1	0	5.57836	-4.43384	3.52128
65	6	0	0.26687	1.44711	-4.20794
66	1	0	-0.36399	2.08792	-4.8423
67	6	0	2.8097	-2.10691	0.57736
68	6	0	4.2976	-3.34371	2.18372
69	6	0	-2.57054	-3.68805	-1.50792
70	6	0	-3.92686	0.26818	-0.86563
71	1	0	-4.86349	0.83211	-0.90982
72	6	0	-4.19824	3.33603	1.06457
73	6	0	1.38836	0.82911	-4.74331
74	1	0	1.65599	0.9799	-5.79923
75	6	0	5.67801	-4.55659	0.11913
76	1	0	6.21709	-5.01934	-0.71642
77	6	0	-5.80589	4.74977	-0.00125
78	1	0	-6.67807	5.4149	0.06125
79	6	0	5.07651	5.95501	-0.3595
80	1	0	5.76844	6.79746	-0.49513
81	6	0	4.59932	5.27661	-1.4677
82	1	0	4.89765	5.55885	-2.48461
83	6	0	2.16627	0.01675	-3.934
84	1	0	3.05433	-0.48699	-4.34492
85	6	0	-4.10503	-5.77862	-2.58397
86	1	0	-4.70507	-6.59715	-3.00417
87	6	0	-4.02885	-5.62073	-1.21138
88	1	0	-4.55948	-6.29373	-0.52701
89	8	0	-0.23653	0.25511	1.66348
90	6	0	-0.27982	-1.86883	3.95813
91	6	0	-1.36904	-1.49509	3.01492
92	1	0	0.60757	-2.22609	3.40475
93	1	0	0.05611	-1.02134	4.58334
94	1	0	-0.58838	-2.68137	4.64788
95	1	0	-0.88343	-0.5822	2.32545
96	1	0	-1.52719	-2.24944	2.21626
97	6	0	-2.63771	-0.9678	3.51125
98	6	0	-2.75149	-0.3253	4.75133
99	6	0	-3.78996	-1.06305	2.71653
100	6	0	-3.96652	0.17415	5.18529
101	1	0	-1.86639	-0.2211	5.3942
102	6	0	-5.00206	-0.56333	3.15146
103	1	0	-3.72122	-1.56213	1.7376
104	6	0	-5.09908	0.05525	4.39118
105	1	0	-4.03256	0.66514	6.16681
106	1	0	-5.89186	-0.66128	2.51337
107	1	0	-6.06316	0.45219	4.73899

### TS2 ( $S = 1/2$ )

Center Number	Atomic Number	Atomic Type	X	Y	Z
1	17	0	-2.71536	-4.64147	1.94782

2	17	0	-4.33313	1.61328	2.60349
3	17	0	1.89024	4.04165	-2.84884
4	17	0	1.40123	4.74314	2.44913
5	17	0	-4.90337	2.05017	-2.70776
6	7	0	0.47366	-1.84369	0.23158
7	7	0	1.58427	0.78226	0.35374
8	7	0	-2.09965	-0.76668	-0.30379
9	7	0	-1.00844	1.9053	-0.15403
10	17	0	-1.30628	-4.12629	-3.21164
11	17	0	2.23311	-1.24836	4.03922
12	17	0	5.18543	-2.19598	-0.3335
13	6	0	-2.31164	2.23167	-0.18467
14	6	0	-0.29716	3.04478	-0.2263
15	6	0	1.68308	-2.16079	0.76641
16	6	0	-0.77969	0.26547	1.97148
17	6	0	-2.44963	3.65762	-0.27055
18	1	0	-3.3954	4.20578	-0.31351
19	6	0	2.65425	0.1133	0.82649
20	6	0	1.68712	4.49206	-0.21346
21	6	0	-0.18788	-3.01151	0.01599
22	6	0	1.94797	2.07944	0.21067
23	6	0	2.68107	-1.25397	1.10848
24	6	0	-3.37102	1.32054	-0.19058
25	6	0	-1.36057	-0.8252	2.62884
26	1	0	-1.62669	-1.74247	2.07913
27	6	0	-3.25593	-0.06355	-0.31072
28	6	0	-4.73423	1.87605	-0.03715
29	6	0	3.7614	1.00941	0.97339
30	1	0	4.75872	0.73411	1.32975
31	6	0	1.09349	3.13745	-0.10335
32	6	0	1.79255	-3.5791	0.89169
33	1	0	2.6605	-4.11272	1.29086
34	6	0	0.64566	-4.10854	0.39296
35	1	0	0.37439	-5.16582	0.31363
36	6	0	-3.83189	-2.19979	-0.65096
37	1	0	-4.36388	-3.13971	-0.82677
38	6	0	-2.03275	-4.48935	-0.64798
39	6	0	-2.41543	-2.06359	-0.48763
40	6	0	3.68134	-1.81752	3.31165
41	6	0	4.69291	-2.31547	4.11952
42	1	0	4.55248	-2.33633	5.20705
43	6	0	-1.19321	4.16341	-0.32239
44	1	0	-0.89761	5.2138	-0.40256
45	6	0	-2.60098	-5.27533	0.35733
46	6	0	1.86228	5.31972	0.89794
47	6	0	-4.35771	-0.95735	-0.51036
48	1	0	-5.41131	-0.66638	-0.55809
49	6	0	-2.99376	-7.0713	-1.16771
50	1	0	-3.36984	-8.08354	-1.36999
51	6	0	4.99634	-2.245	1.36866
52	6	0	2.39562	6.59556	0.79504
53	1	0	2.5086	7.20583	1.69928
54	6	0	-5.52799	2.24646	-1.12263
55	6	0	2.61796	6.28346	-1.57821
56	1	0	2.91162	6.64433	-2.57155
57	6	0	-5.27485	2.05564	1.24021
58	6	0	-6.8022	2.77032	-0.95688
59	1	0	-7.39071	3.0469	-1.84009
60	6	0	-0.4949	1.40407	2.72521

61	1	0	-0.0615	2.29662	2.25019
62	6	0	-2.4436	-6.32647	-2.19561
63	1	0	-2.37362	-6.72169	-3.21597
64	6	0	-0.74086	1.44168	4.0898
65	1	0	-0.49859	2.35012	4.6615
66	6	0	-1.51519	-3.12682	-0.39083
67	6	0	-1.97329	-5.05025	-1.92615
68	6	0	3.8056	-1.77057	1.91877
69	6	0	3.33038	2.2272	0.5592
70	1	0	3.89857	3.16148	0.51791
71	6	0	2.08009	5.01105	-1.44983
72	6	0	-1.29407	0.34274	4.73232
73	1	0	-1.49584	0.37484	5.81287
74	6	0	-3.07907	-6.55382	0.11289
75	1	0	-3.51668	-7.13169	0.93557
76	6	0	2.7706	7.0693	-0.44981
77	1	0	3.19434	8.07852	-0.54377
78	6	0	-7.30108	2.93161	0.32422
79	1	0	-8.30842	3.34691	0.46448
80	6	0	-6.54629	2.57758	1.42937
81	1	0	-6.9298	2.70116	2.4492
82	6	0	-1.601	-0.79116	3.99581
83	1	0	-2.04397	-1.66896	4.48993
84	6	0	5.85812	-2.778	3.53271
85	1	0	6.66418	-3.17429	4.16547
86	6	0	6.02156	-2.74552	2.1586
87	1	0	6.94046	-3.10866	1.68258
88	8	0	1.18247	1.17569	-3.9423
89	6	0	0.60798	-1.05687	-4.58701
90	6	0	1.39471	-0.1494	-3.68758
91	1	0	-0.4525	-0.75311	-4.58426
92	1	0	0.97325	-0.99366	-5.63148
93	1	0	0.65007	-2.11229	-4.26555
94	1	0	0.42118	1.42236	-3.40404
95	1	0	0.88196	-0.30192	-2.60467
96	6	0	2.83916	-0.43308	-3.50891
97	6	0	3.65475	0.55007	-2.93652
98	6	0	3.42466	-1.64476	-3.88394
99	6	0	5.01341	0.34287	-2.78987
100	1	0	3.19638	1.50184	-2.63106
101	6	0	4.78722	-1.84779	-3.73876
102	1	0	2.81173	-2.43963	-4.33032
103	6	0	5.58967	-0.85115	-3.20389
104	1	0	5.63928	1.13149	-2.34783
105	1	0	5.23274	-2.7993	-4.06217
106	1	0	6.67226	-1.01079	-3.09627
107	44	0	-0.24583	-0.00217	-0.02632
108	8	0	-0.0498	0.27469	-1.78037

### TS3 ( $S = 1/2$ )

Center Number	Atomic Number	Atomic Type	Coordinates (Angstroms)		
			X	Y	Z
1	44	0	0.03471	0.09333	0.07739
2	17	0	4.85926	-1.26587	-2.18084
3	17	0	0.98266	4.02165	-3.10929

4	17	0	-4.13314	1.3125	3.06714
5	17	0	-4.99022	1.31817	-2.22946
6	17	0	1.55047	5.25082	2.08224
7	7	0	1.04047	-1.63828	-0.01502
8	7	0	-1.72192	-0.90883	-0.12232
9	7	0	1.78093	1.09825	0.158
10	7	0	-0.99668	1.86648	0.01034
11	17	0	4.42634	-1.00719	3.1722
12	17	0	-0.55263	-3.16959	-3.6067
13	17	0	-1.71453	-5.42667	1.12505
14	6	0	-0.46085	3.08791	-0.12292
15	6	0	-2.32524	2.01252	0.15851
16	6	0	0.52362	-2.84033	-0.38722
17	6	0	0.02912	0.34192	-1.98312
18	6	0	-1.50043	4.07949	-0.08183
19	1	0	-1.35375	5.16056	-0.1665
20	6	0	-1.87012	-2.20682	-0.44599
21	6	0	-4.66819	1.33815	0.43847
22	6	0	2.37467	-1.81604	0.16615
23	6	0	-2.95692	-0.38607	0.04466
24	6	0	-0.81734	-3.10184	-0.65828
25	6	0	0.90777	3.35791	-0.211
26	6	0	1.22879	0.10069	-2.66124
27	1	0	2.15021	-0.14006	-2.10814
28	6	0	1.93479	2.43255	-0.02998
29	6	0	1.29259	4.74863	-0.54302
30	6	0	-3.26309	-2.54127	-0.48144
31	1	0	-3.67618	-3.52737	-0.71391
32	6	0	-3.24904	0.96741	0.2308
33	6	0	1.56195	-3.82167	-0.40833
34	1	0	1.43002	-4.87791	-0.66191
35	6	0	2.70561	-3.19296	-0.03367
36	1	0	3.70526	-3.62603	0.06991
37	6	0	3.99683	1.60888	0.25958
38	1	0	5.07703	1.46795	0.3636
39	6	0	4.72935	-1.18064	0.5069
40	6	0	3.01445	0.56906	0.31355
41	6	0	-1.04293	-4.52925	-2.68147
42	6	0	-1.33452	-5.7204	-3.33008
43	1	0	-1.24396	-5.77366	-4.42169
44	6	0	-2.66045	3.41004	0.12256
45	1	0	-3.66782	3.82557	0.22384
46	6	0	5.53583	-1.42208	-0.61072
47	6	0	-5.55515	1.52955	-0.6234
48	6	0	3.32651	2.76438	0.02123
49	1	0	3.74452	3.76888	-0.09585
50	6	0	7.43492	-1.89366	0.76013
51	1	0	8.49207	-2.17499	0.85957
52	6	0	-1.56113	-5.52671	-0.58232
53	6	0	-6.88044	1.88633	-0.42381
54	1	0	-7.53726	2.02475	-1.29108
55	6	0	1.59953	5.70446	0.42614
56	6	0	-6.49833	1.88797	1.95111
57	1	0	-6.85009	2.0255	2.98087
58	6	0	1.3458	5.15902	-1.87868
59	6	0	1.94019	7.00757	0.09475
60	1	0	2.16992	7.72372	0.89298
61	6	0	-1.09635	0.6582	-2.74483
62	1	0	-2.06259	0.86316	-2.25827
63	6	0	6.67942	-1.65456	1.89426

64	1	0	7.11242	-1.73619	2.89854
65	6	0	-1.03448	0.7114	-4.12965
66	1	0	-1.94018	0.95475	-4.70526
67	6	0	3.30374	-0.79668	0.37414
68	6	0	5.34489	-1.30276	1.75474
69	6	0	-1.14321	-4.40032	-1.2906
70	6	0	-3.93804	-1.41553	-0.13696
71	1	0	-5.0204	-1.28443	-0.04248
72	6	0	-5.17766	1.52875	1.72554
73	6	0	0.16035	0.4569	-4.78816
74	1	0	0.21005	0.50042	-5.88583
75	6	0	6.87178	-1.77781	-0.49818
76	1	0	7.45881	-1.95716	-1.40667
77	6	0	-7.34266	2.06322	0.86868
78	1	0	-8.39029	2.34822	1.03633
79	6	0	1.97948	7.3731	-1.23963
80	1	0	2.24762	8.40284	-1.51312
81	6	0	1.68612	6.45599	-2.23374
82	1	0	1.71548	6.7321	-3.29448
83	6	0	1.29127	0.1493	-4.04723
84	1	0	2.24649	-0.05259	-4.55573
85	6	0	-1.74005	-6.81388	-2.58527
86	1	0	-1.97348	-7.7601	-3.09249
87	6	0	-1.85892	-6.72762	-1.20926
88	1	0	-2.18034	-7.58579	-0.60644
89	8	0	-0.38472	0.33823	1.82812
90	6	0	1.09406	0.373	4.54645
91	1	0	0.64518	1.3817	4.57429
92	1	0	2.01682	0.4339	3.93993
93	1	0	1.40389	0.12222	5.58456
94	6	0	0.14754	-0.64124	4.00984
95	6	0	0.71839	-2.01105	3.79827
96	6	0	-1.2257	-0.63457	4.61109
97	1	0	-0.07756	-0.22083	2.83939
98	6	0	-0.25405	-2.96758	3.15223
99	1	0	1.0277	-2.40547	4.79924
100	1	0	1.66168	-1.94654	3.21657
101	6	0	-2.17363	-1.60324	3.94244
102	1	0	-1.63277	0.39785	4.60153
103	1	0	-1.12611	-0.89678	5.69451
104	6	0	-1.58371	-2.99044	3.86512
105	1	0	0.18823	-3.98157	3.08924
106	1	0	-0.41883	-2.65044	2.10133
107	1	0	-3.14839	-1.61068	4.46867
108	1	0	-2.39309	-1.24024	2.91302
109	1	0	-1.45324	-3.40041	4.89248
110	1	0	-2.28609	-3.67901	3.35453